

**Measuring irradiance, temperature and angle of incidence effects on  
photovoltaic modules in Auburn Hills, Michigan**

by

Michael S. Buday

A practicum submitted  
in partial fulfillment of the requirements  
for the degree of  
Master of Science/Sustainable Systems  
(Natural Resources and Environment)  
at the University of Michigan  
August 2011

Advisors

Professor Gregory Keoleian, Chair

Bill Marion, Principal Scientist and Project Leader of Photovoltaic Research NREL

## Contents

Abstract.....	iii
Acknowledgments.....	iv
Introduction .....	1
Literature Review.....	3
Methods.....	8
Results.....	15
Conclusion.....	20
Glossary.....	22
References .....	24
Appendices.....	27

## List of Tables

Table 1: IEC 61853-1 Matrix-based test conditions.....	1
Table 2: Modules under test.....	14
Table 3: Trends in power by PV material.....	15
Table 4: Power at 1000W/m <sup>2</sup> by PV material.....	16
Table 5: Observations fitting IEC 61853-1 parameters.....	19

## List of Figures

Figure 1: Impacts of temperature coefficients on PV power.....	4
Figure 2: Solar spectra measurements and line fit from one day from existing literature .....	5
Figure 3: Calculated mismatch factor for a-Si module from existing literature .....	6
Figure 4: System diagram.....	8
Figure 5: Sample IV-curve .....	9
Figure 6: K12430 I-V Characteristics pulse mode .....	10
Figure 7: Four-wire connection.....	10
Figure 8: KI#7053 Switch-card connection for 5<A<8.....	11
Figure 9: KI#7053 Switch-card with soldered leads .....	11
Figure 10: Fixed resistor board .....	12
Figure 11: Test equipment.....	12
Figure 12: GPIB (IEEE-488) .....	12
Figure 13: Project timeline.....	13
Figure 14: Power vs POA Irradiance for a-Si, c-Si and CIGS modules .....	16
Figure 15: Temperature corrected P <sub>max</sub> c-Si.....	17

## Abstract

United Solar Ovonic (USO) installed a photovoltaic (PV) module testing system in Auburn Hills, Michigan (Latitude 42.6978, Longitude -83.2419) in March of 2010 for the purpose of evaluating the impacts of irradiance, temperature and angle of incidence (AOI) effects on PV module performance. We considered various test-bed designs and ultimately, constructed a source-meter-based current and voltage measurement system coupled with a data acquisition system recording readings from weather-station instruments that track solar irradiance, temperature and wind speed. Current, voltage and power observations, correlated to our weather-station device readings, were collected from commercially available PV modules manufactured from mono-crystalline silicon (c-Si), amorphous silicon (a-Si) and copper indium gallium selenide (CIGS). We observed thermal annealing in a-Si and the effects of temperature on c-Si and CIGS. c-Si module temperatures above 25°C appear to diminish power by approximately 0.5%/°C. The results were consistent with our expectations based on existing literature. From this, we infer that the test-bed is effective at measuring module performance.

Our results support, but do not confirm the hypothesis that a-Si modules deliver more energy (kWhrs) per peak-watt ( $W_p$ ) than other PV materials. Confirming the hypothesis would require both testing a statistically significant number of PV modules and performing a quantitative analysis of the accuracy of the test-bed. This is important because PV is typically sold on a  $\$/W_p$  basis. The  $W_p$  rating is based on a module's performance under standard test conditions (STC) of 1000W/m<sup>2</sup>, 1.5 air mass (AM) and 25°C module temperature. A new PV rating system proposed by the International Electrotechnical Commission (IEC) creates a series of testing conditions based on a variety of weather conditions. USO's PV measurement system is capable of collecting observations fitting most, but not all of these test conditions. Due to the array's northern location, none of our observations fit the IEC's high temperature conditions.

## **Acknowledgments**

This project was made possible through sponsorship by United Solar Ovonic (USO) and its Chairman Subhendu Guha. I am very grateful for the opportunity that he gave me. I worked under the direct supervision of USO Senior Research Scientist, Kevin Beernink. His guidance, instruction, support and participation were critical to the success of the project. I also received help from many other USO employees, most notably, Chris Worrel, David Wolf, Greg Dimaggio, Logan Rowe, Ginger Pietka, Kias Younan, Eric Ahkashian, Brent Batchelder, Mike Ondocsin, Tony Turkin, Mike Walters, and Jacob Washington.

Joseph del Cueto, Bill Marion and Daryl Myers, all at the National Renewable Energy Laboratory (NREL) hold a rare level of expertise in this field. Their publications, guidance and feedback were vital to the development of this report.

Timothy Dierauf, Adrienne Kimber and John Previtali submitted presentations at the American Solar Energy Society's 2011 national conference and provided me with reference materials. Through their work, they have further demonstrated the importance of this field of research in industry.

Sondra Auerbach, Jennifer Taylor and Diana Woodworth in the School of Natural Resources and Environment's (SNRE) Office of Academic Programs welcomed me to the SNRE community and facilitated my education. Outside of SNRE, Professor Debra Rowe, Robert Pratt, David Lankheet and Professor Ian Hiskens were my key teachers in this discipline. These people all helped put me on this track, making this report possible.

SNRE Professor and Co-Director of the Center for Sustainable Systems Gregory Keoleian was instrumental in approaching USO regarding an internship and master's project. The time he has spent teaching and meeting with me over the past three years has been invaluable to both this project and my education. He devoted a significant amount of time to overseeing this project and contributing to the content and structure of this report. Helaine Hunscher, Program Coordinator at the Center for Sustainable Systems, also provided vital feedback.

Donna and Joseph Napolitano gave me my first job in the solar industry. They have always encouraged me to learn and to apply what I learn. The SNRE, Erb Institute and Great Lakes Renewable Energy Association communities also provided me with collaborative learning environments.

Finally, I would like to thank my parents, Edna and Gene, for their unconditional support and encouragement through a lengthy career transition.

## Introduction

Photovoltaic (PV) module and array performance is difficult to predict due to variations in weather, air mass (AM), and non-linear performance characteristics of various module technologies. Manufacturers, distributors and developers typically sell PV on a cost per peak-watt ( $\$/W_p$ ) basis. A module's  $W_p$  rating, also known as its  $P_{max}$ , is based on its performance under Standard Test Conditions (STC) consisting of  $1000W/m^2$ , 1.5 AM and  $25^\circ C$  module temperature. However, these conditions rarely occur simultaneously in nature and the performance of PV materials varies over time and by geographic location based primarily on differences in temperature and AM (Marion, Kroposki, Emery, del Cueto, Myers, & Osterwald, 1999). The International Electrotechnical Commission (IEC) has proposed PV rating standards (IEC 61853) that include characterizing module performance based on a matrix of various weather conditions, including high temperature conditions (HTC), STC, nominal operating cell temperature (NOCT), low temperature conditions (LTC) and low irradiance conditions (LIC). The criteria for these conditions appear in Table 1 below. Note that IEC 61853-1 does not include evaluating performance under photovoltaics for utility scale applications test conditions (PVUSA or PTC) of  $1000W/m^2$ ,  $20^\circ C$  ambient temperature, wind speed of 1 meter/second and 1.5 AM.

**Table 1: IEC 61853-1 Matrix-based test conditions**

Abbrev.	Description	Irradiance ( $W/m^2$ )	Module Temp. ( $^\circ C$ )	Ambient Temp. ( $^\circ C$ )	Wind Speed (m/sec)	AM
HTC	High temperature conditions	1000	75			1.5
STC	Standard test conditions	1000	25			1.5
NOCT	Nominal operating cell temperature	800		20	1	1.5
LTC	Low temperature conditions	500	15			1.5
LIC	Low irradiance conditions	200	25			1.5

With its proposed ratings standards, the IEC seeks to improve the method by which PV module performance is evaluated by measuring PV power under a set of testing conditions, instead of only STC. The standards also establish guidelines for rating PV based on energy yield (watt-hours) and performance ratio (PR) (Poissant, Pelland, & Turcotte, 2008) (del Cueto, 2007).

Advances in inverter technology have reduced the cost of PV array performance monitoring substantially, to less than \$1000 or to 1%-10% of overall system cost for a 1-

20kW grid-tied system (Enphase Energy, 2011) (Fronius USA LLC, 2011). This is within reach of many homeowners installing PV systems. These monitoring systems report on an array's energy yield. However, these systems do not provide the level of information acquired from performing a full current-voltage (IV) sweep. They also do not include weather stations. The equipment required to effectively analyze the electrical characteristics of PV modules and arrays as well as the effects of irradiance and module temperature ranges between \$10,000 and \$50,000 (not including the modules themselves). To better understand and predict PV system performance, NREL's Performance and Energy Rating Test-bed (PERT) and Outdoor Testing Field (OTF) go beyond performing basic energy yield and power rating measurements. Research scientists at NREL designed systems with the ability to examine the electrical and optical-response characteristics of various production modules and prototypes over time.

Michigan-based PV module manufacturer, United Solar Ovonic (USO) sought to develop a system with PV module test capabilities similar to NREL's stand-alone testing system in order to conduct their own characterization of competitor's modules and USO's next generation of products on a fraction of NREL's budget. The system went live in March of 2010 and continues to perform and record regular measurements (IV sweeps) on 20 PV modules every ten minutes during daylight-hours. It also records basic meteorological conditions with each sweep, including plane of array (POA) irradiance, ambient and module temperature, and wind speed. We collected and bundled field observations into the standard's categories representing various weather conditions in order to verify the capability of USO's measurement system to test IEC 61853-1.

Once we designed and installed our PV module testing system and began collecting data, we then had the information needed to evaluate module energy production as well as the electrical and basic optical response characteristics of the various PV modules under test. We applied our test method and found results consistent with our expectations based on existing literature, which is highlighted in the next section. In this paper, we report on the relationships we found between power and irradiance as well as between power and module temperature based on observations taken from select amorphous silicon (a-Si), crystalline silicon (c-Si), and copper indium gallium selenide (CIGS) modules from July through December of 2010. (Observations from December 14<sup>th</sup> through 20<sup>th</sup> were ignored because many of the modules were covered in snow.) We were unable to obtain cadmium-telluride (CdTe) modules due to the manufacturer's tight control of its distribution channel.

Given that power is the product of voltage (V) and current (I), the proposed standard calls for evaluating open-circuit voltage ( $V_{oc}$ ) and short-circuit current ( $I_{sc}$ ), and

fill-factor (FF) against both irradiance and module temperature (del Cueto, 2007). FF indicates a module's relative efficiency. We designed and built a system capable of measuring all of these parameters and others including  $V_{mp}$ . (Many of these relationships appear in Appendices 5 through 7.) However, the measurement system is not 100% accurate. There is a level of uncertainty in the data it generates.

## Literature Review

Thirty years ago, researchers in the PV field acknowledged the need to go beyond STC, suggesting that module performance be characterized by categories of weather conditions (hot sunny, cold sunny, hot cloudy, cold cloudy, and nice) (Marion, Kroposki, Emery, del Cueto, Myers, & Osterwald, 1999) (Gay, Rumberg, & Wilson, 1982). The IEC's current proposed standard seeks to address this need (del Cueto, 2007).

The main purpose of the literature review was to examine existing research in order to identify the key variables affecting PV power generation and to determine how to measure those variables effectively. Existing literature was helpful in establishing our system architecture, in defining performance metrics and in identifying areas of opportunity for further learning. We sought to develop measurement and testing capabilities approaching those of a well-funded government laboratory and so focused our research on publications from NREL and Sandia Labs. We also reviewed articles relating to performance analysis of installed PV arrays ranging in size from 2-500 kW<sub>p</sub>.

Irradiance has the greatest impact on PV power. Beyond irradiance, module temperature, angle of incidence (AOI) and AM also affect a module's or an array's power and production (del Cueto, 2007) (Myers, 2009) (King, Kratochvil, & Boyson, 1997). Module temperature is in turn, influenced by ambient temperature, cloud patterns and wind speed. Researchers have used sophisticated testing and measurement devices in PV performance testing for over 30 years, yet predicting module performance remains complex and forecasters must accept a relatively high level of uncertainty in predicting energy production from a PV array. Additionally, under rapidly changing and extreme weather conditions, inverter ramp-times and clipping both diminish AC power generation (van Cleef, Lippens, & Call, 2001) .

Researchers use pyranometers to measure irradiance, but there are different classes of pyranometers. Secondary-standard and first-class thermopile-type pyranometers measure irradiance throughout the range of frequencies to which PV responds (300-2800nm). Silicon diode pyranometers only respond to a narrower range of frequencies (400-1100nm), but are still used in PV weather stations because they are less expensive than thermopiles and because they are actually more sensitive than

thermopiles in the range of frequencies to which they do respond. Furthermore, silicon-based PV is also primarily responsive within this range.

Measuring module temperature is important because c-Si and other PV materials produce less power at high temperatures. Figure 1 (below) indicates the impacts of module temperature on various PV materials. Estimating module temperature is achieved with the use of a thermocouple attached to the back of the module. However, under most conditions, the module temperature is likely to be warmer than the back of the module. Furthermore, the temperature of the module is not likely to be consistent throughout its entire surface. For these reasons, researchers apply a standard adjustment to the back of the module temperature reading to compensate for the temperature difference between the back of the module and surface of the module and they may place more than one thermocouple in several specific positions on the back of a module in order to calculate an average temperature.

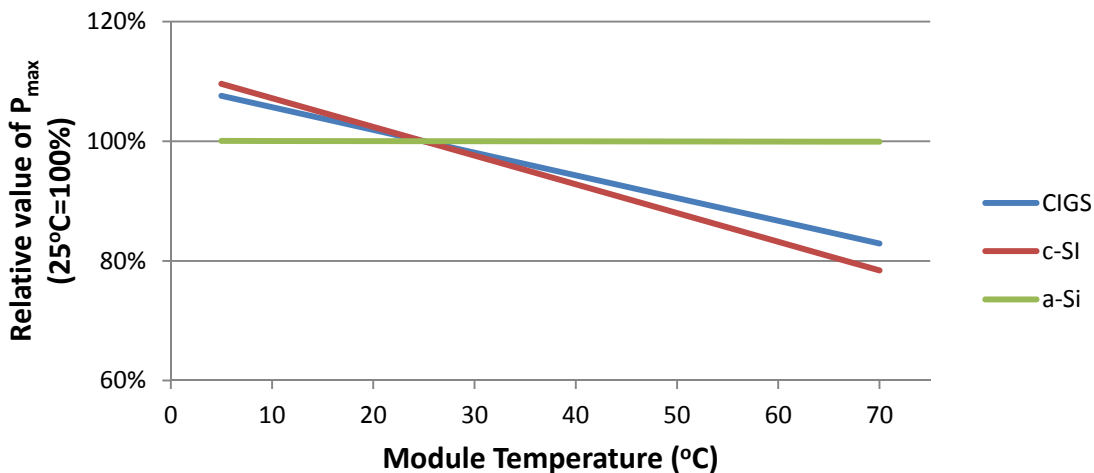


**Figure 1: Impacts of temperature coefficients on PV power**

A high AOI can significantly reduce PV power generation. Reda and Andreas provided the solar position algorithm (Reda & Andreas, 2008) we used to find zenith, declination, and azimuth angles required to calculate AOI in order to plot it against  $\%P_{\max}$  and other variables.

PV performance is typically reported to AM1.5. (This value was chosen because it represents the average AM at solar noon for optimally tilted PV arrays at latitudes in the continental US.) AM1.5 reference (or standard) refers to the relative path length of the direct sunlight through the atmosphere. With the sun directly overhead (zenith) AM is 1.0 (uncorrected). With longer path lengths, there is more scattering and absorption of solar radiation by atmospheric constituents such as water vapor and aerosols. Similar to



solar spectrum (King, Kratochvil, & Boyson, 1997), both AM and atmospheric conditions vary with time, date, and location (Riordan & Hulstron, 1990).

When the actual solar spectrum deviates from AM1.5 or the spectral response of the PV differs from the reference device (i.e., the pyranometer), the impact of AM on PV module or array performance is stated as a spectral mismatch factor (K) (Kenny, Ioannides, Mullejans, & Dunlop, 2004). Figure 2 (below) illustrates the increase in K with increasing AM. Figure 3 (below) exhibits irradiance density by wavelength based on a study by Kenny et al.

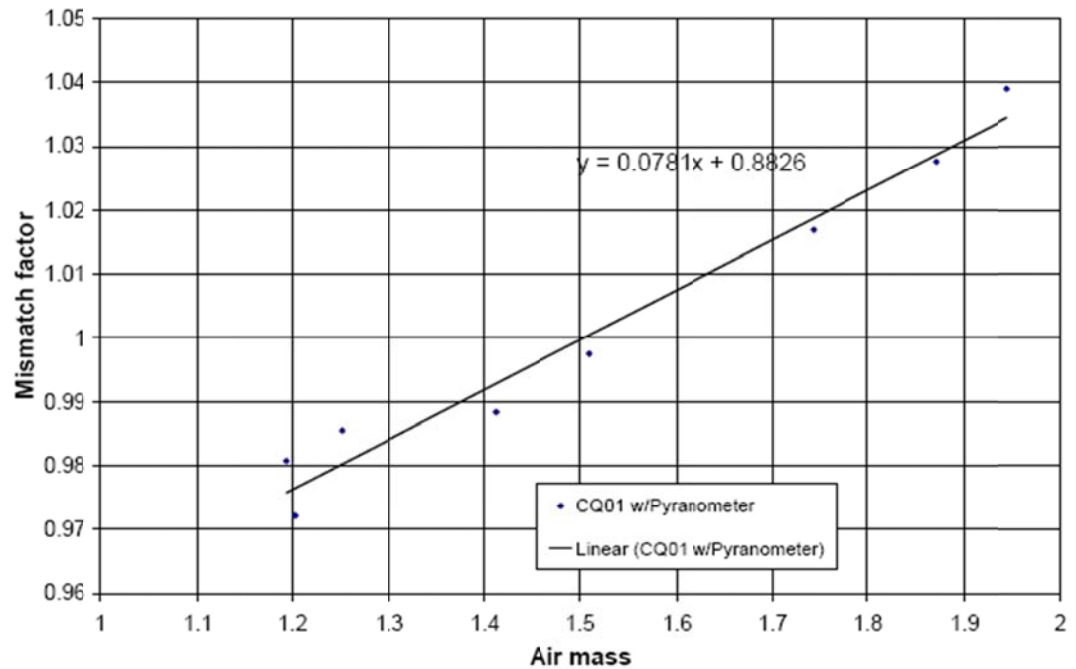


**Figure 2: Solar spectra measurements and line fit from one day from existing literature** (Kenny, Ioannides, Mullejans, & Dunlop, 2004)

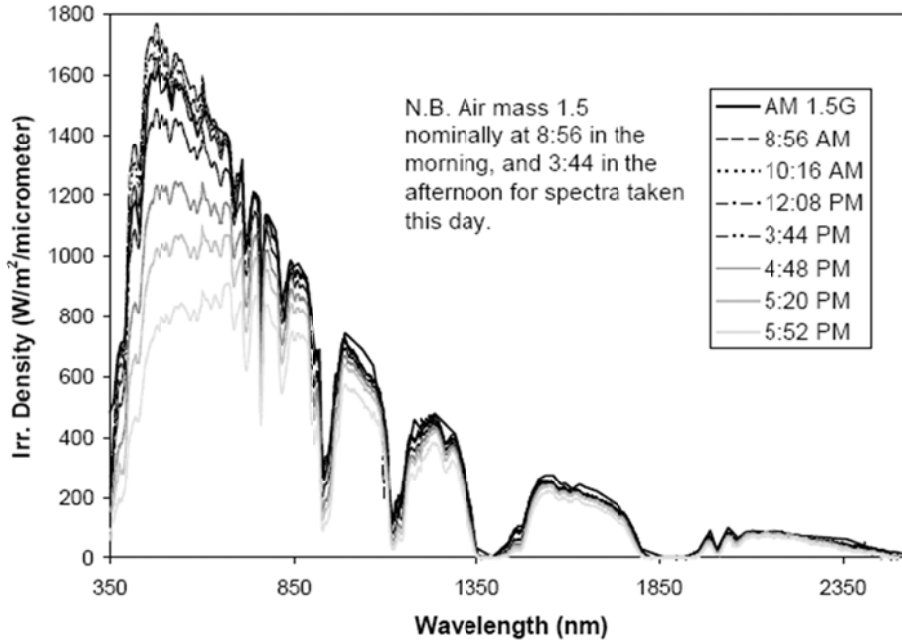


**Figure 3: Calculated mismatch factor for a-Si module from existing literature**  
(Kenny, Ioannides, Mullejans, & Dunlop, 2004)

Our work did not include correcting for spectral mismatch and the USO system's commercial photodiode pyranometers cannot measure spectral irradiance above 1100nm, adding uncertainty into the results. However, in "Spectral Corrections Based on Optical Air Mass", Keith Emery, Joseph DelCueto, and Willem Zaaiman offer a spectral correction factor derived from a polynomial fit of  $I_{SC}$  measured under natural sunlight divided by the full spectrum irradiance as a function of air mass (Emery, DelCueto, & Zaaiman, 2003). The equation can be written as:

**Equation 1**

$$CV = \frac{I_{sc}}{E_{tot}} \times \frac{\int_{0.3\mu m}^{4.0\mu m} E_R(\lambda) S_T(\lambda) d\lambda}{\int_{0.3\mu m}^{4.0\mu m} E_R(\lambda) S_R(\lambda) d\lambda} \times \frac{\int_{0.3\mu m}^{4.0\mu m} E_S(\lambda) S_R(\lambda) d\lambda}{\int_{0.3\mu m}^{4.0\mu m} E_S(\lambda) S_T(\lambda) d\lambda}$$

where  $E_{tot}$  is the total irradiance,  $E_R(\lambda)$  is the spectral irradiance of the reference spectrum,  $E_S(\lambda)$  is the spectral irradiance of the solar spectrum,  $S_R(\lambda)$  is the spectral responsivity of the reference detector, and  $S_T(\lambda)$  is the spectral responsivity of the test device with measured short-circuit current  $I_{sc}$  (Emery, DelCueto, & Zaaiman, 2003). They found that using a matched reference cell to measure total irradiance reduces uncertainty in spectral correction but makes the correction equation dependant on the detector employed and the air mass based spectral correction factor is both location and time dependent. In their paper, they also noted that a-Si is much more

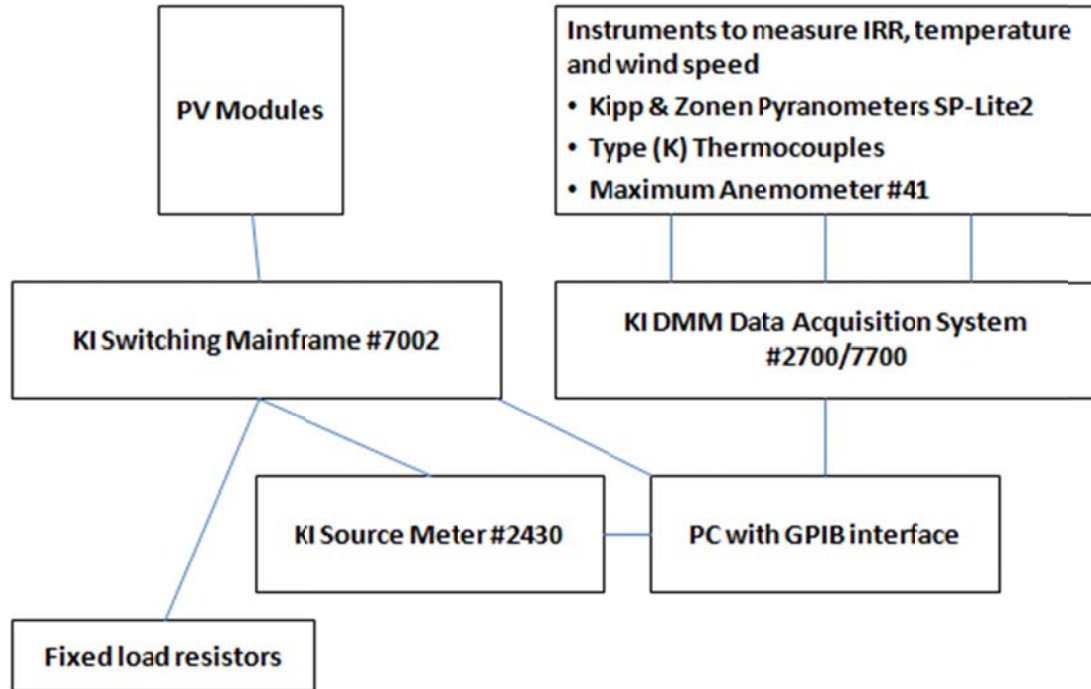
sensitive to water vapor and turbidity than c-Si, CIGS and CdTe. As stated previously our system does not include a CdTe module under test because of the manufacturer's tightly controlled distribution channel. Instead, we relied on existing literature to provide a basic comparison to the results we found for c-Si, a-Si and CIGS modules (del Cueto, 2007).

We also recorded wind speed and ambient temperature with each module's IV sweep, even though Myers showed no strong correlation between power and either wind speed or ambient temperature (Myers, 2009).

The literature also provided a basis for understanding the level of uncertainty we could expect from our analysis. There are several sources of uncertainty including a lack of precision in the measurement devices and rapidly changing conditions (e.g., irradiance) during test periods. The precision ratings of our measurement devices are available in Appendix 1. During one experiment conducted in 1998, Marion at NREL found that "Because of errors in measurements and energy-rating methodology, differences of 8% or less in the energy ratings of two PV modules are not significant. If one of the modules is a-Si, differences of 13% or less in the energy ratings of two PV modules are not significant." (Marion, 2000)

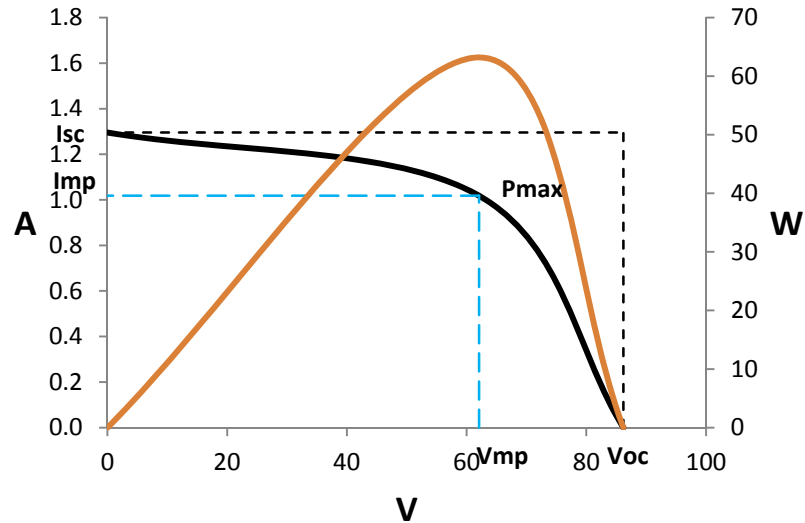
## Methods

Figure 4 shows the key elements of the measurement system including the connections between the PV modules under test and the measurement devices and other components within the test-bed.



**Figure 4: System diagram**

The heart of the test-bed is a 1kW Keithley Instruments (KI) model#2430 source-meter. Measurements of a module's power are obtained by sourcing current to the module under test while sensing its voltage. The source-meter conducts an IV sweep by first finding  $V_{OC}$  (where  $I=0$ ). The software then instructs the source-meter to increase current at such an interval to allow for approximately 80 points or steps before the voltage reads zero (which occurs at  $I_{sc}$ ). The result is an IV curve with  $P_{max} = I_{mp} \times V_{mp} = I_{sc} \times V_{oc} \times FF$ , where the product  $I_{sc} \times V_{oc}$  represents the module's theoretical maximum power and FF reflects its relative efficiency, as shown in Figure 5 below.



**Figure 5: Sample IV-curve with Y-axis A (left) and Power-curve with Y-axis W (right)**

Note that the illustration above shows a standard first quadrant IV curve, but that the system in fact carries out fourth quadrant sweeps. In addition to  $V_{oc}$  and  $I_{sc}$ , the file also records  $P_{max}$  (the point at which the product of  $V \times I$  reaches its maximum power value),  $FF [ = (V_{mp} \times I_{mp}) / (V_{oc} \times I_{sc}) ]$  and a timestamp. The system initiates an IV sweep every ten minutes when irradiance is greater than  $20W/m^2$  (2% of full-sun). This is not as fine a resolution as some other monitoring systems (e.g., NREL's OTF) which take measurements every minute or even more frequently.

Alternated with its sweeps, the software calls for readings from devices connected to the data acquisition system, namely a Maximum model #41 three-cup anemometer, type-K thermocouples attached to the back of each module and two ambient points (shaded and not shaded), and several Kipp and Zonen SPLite2 photodiode detector pyranometers. We also added a secondary standard Kipp and Zonen CMP-21 thermopile in March 2011. As previously stated, all of the other findings in this report are based on observations taken between July and December 2010. However, the findings based on CMP-21 measurements were taken between March and July 2011. (The measured correlation between a SPLite2 and the CMP-21 appears in Appendix 2.) However, the CMP-21 was calibrated by the manufacturer and not put through NREL's more rigorous calibration process (Emery, et al., 2005) (Device Performance, 2006).

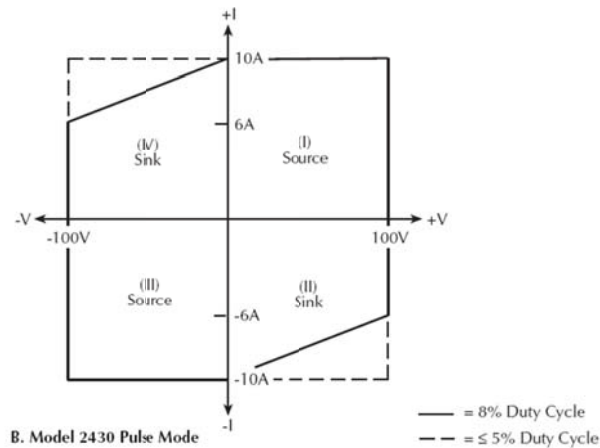


**Figure 6: K12430 I-V Characteristics pulse mode**

*Four-wire connections (remote sense)*

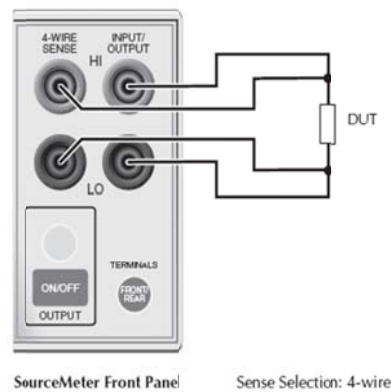


**Figure 7: Four-wire connection**

The KI#2430 is capable of sourcing or sensing up to  $\pm 10$  A and  $\pm 100$  Vdc in pulse mode with a four-wire connection. Figure 6 (above) indicates the source and sink characteristics of our source-meter in pulse mode. Figure 7 (above) shows the source-meter four-wire connection. (We set our pulse width at 0.0025 milliseconds and our pulse delay at 0.05 milliseconds.) However, the system's KI#7053 switching cards can only handle up to 4 A. We were able to double the switching cards' tolerance to 8 A by splitting the current between the cards' two channels (H/L). This was important because the  $I_{SC}$  of many PV modules, including some of the modules that we wanted to test, exceeded 3.2 ( $=4/1.25$  safety factor). Splitting the current between the cards' H/L channels allowed the circuit to accommodate the expected maximum current from all of the modules under test, but this was insufficient for testing some high-current modules on the market.

Figure 8 shows the switch-card connection required for current over 4 A. Figure 9 is a photograph of one of our KI#7053 switch-cards with soldered leads.

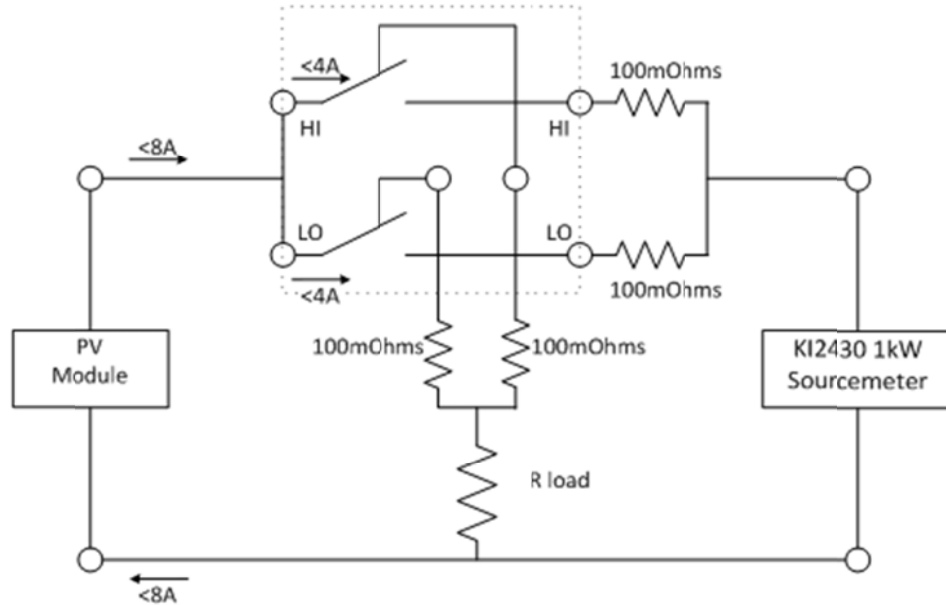


**Figure 8: KI#7053 Switch-card connection for  $4A < I < 8A$**

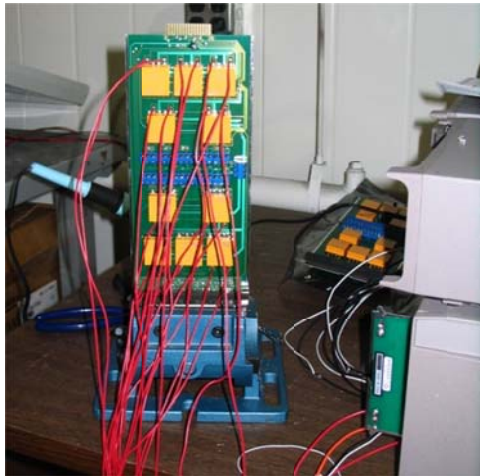


**Figure 9: KI#7053 Switch-card with soldered leads**

Other key components of the system include a 10-slot Keithley Instruments #7002 switching mainframe and a KI#2700 data acquisition system. The switching mainframe directs the system to select a module under test while keeping the other modules routed to fixed load resistors when not under test. Figure 10 shows our fixed

resistor board. The data acquisition system collects readings from the system's thermocouples, pyranometers and anemometer. A list of all system components appears in Appendix 3. System diagrams also appear in Appendix 3.

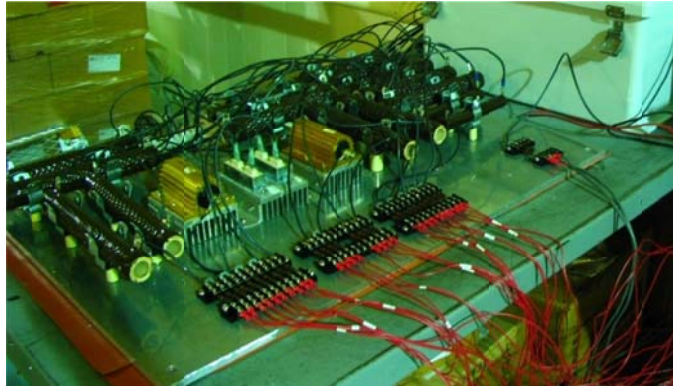


**Figure 10: Fixed resistor board**

All system devices are controlled by a standard personal computer with an IEEE-488 general purpose interface bus (GPIB) and Visual Basic (VB.net) code. From left to right, Figure 11 shows equipment in the test-bed including the resistor board (protected with a cover), junction box, source-meter, switching mainframe and data acquisition. Figure 12 shows GPIB cable ends.



**Figure 11: Fixed resistor board, junction box, source-meter, data acquisition system and switching mainframe**



**Figure 12: GPIB (IEEE-488)**



We considered other system architectures including a curve tracer-based system and grid-tied arrays with inverter-based monitoring systems. The advantages of a Daystar multi-tracer is that it is a turnkey system capable of testing up to sixteen PV modules, 24 thermocouples and eight additional voltage inputs (for pyranometers and other instruments). It would have eliminated the need for a separate data acquisition as well as custom code (Keithley Instruments, 2011). Grid-tied monitoring systems incorporate line and power electronic losses. They assess actual useable AC energy yields. Ultimately, we rejected both of these options for several reasons. Curve tracers are much more expensive than a source-meter system and curve tracers cannot measure  $I_{SC}$  due to unavoidable line losses. Inverter-based monitoring systems do not provide the level of detailed information needed to analyze PV performance effectively.

In addition to rapidly changing conditions during test periods, inaccurate measurement devices influence results. Specifications for the system’s major components appear in Appendix 1. Keithley Instruments #2430 source-meter lists a current source accuracy within 0.045% and a voltage sense accuracy of 0.015%. Specifications for the PV modules under test can be found in Appendix 4.

A timeline of the basic project steps leading to an installed PV module testing system producing data for analysis for this report appears in Figure 13 below:

Task	7/2009	8/2009	9/2009	10/2009	11/2009	12/2009	1/2010	2/2010	3/2010	2010	2010-11
1 Determine & acquire modules to test.				Order	Receive						
2 Determine array location & configuration.											
3 Acquire mounting structure.				Order	Receive						
4 Determine test method.											
5 Determine/acquire hard&software needed.				Order	Receive						
6 Assemble Array.											
7 Configure and Program Test Equipment.											
8 Conduct Measurements.											----->>
9 Compile, tabulate, and interpret data.											----->>

**Figure 13: Project timeline**

From the recorded measurements, we adjusted Vdc instrument readings into calibrated  $W/m^2$  and  $m/sec$  values. We indexed  $P_{max}$  based on the modules’ STC rating using the simple equation:

**Equation 2**

$$\%P_{max} = \frac{\text{measured } P_{max}}{\text{STC rated } P_{max}}$$

We calculated energy yields as:

### Equation 3

$$E_{yield} = \int \text{average } P_{max} \times \text{time lapsed between measurements},$$

with a time increment between measurements set to 10 minutes during daylight hours.

We then indexed power and energy by area (m<sup>2</sup>) and we estimated module temperature as measured back of module temperature plus 3°C per 1000W/m<sup>2</sup>, based on the industry standard.

Influenced by del Cueto's recent study, we reported our results in a series of graphs plotting %P<sub>max</sub>, I<sub>sc</sub>, V<sub>oc</sub> and FF against POA irradiance, as well as %P<sub>max</sub> against AOI, %P<sub>max</sub> and FF against module temperature, and FF and %P<sub>max</sub> over time intervals (del Cueto, 2007). We also calculated linear and polynomial line fits for %P<sub>max</sub> versus irradiance. Finally, using the equation below, we calculated for power correction based on temperature coefficient in order to help assess the impact of module temperature and to estimate the effects of AM and other factors:

### Equation 4

$$\%P_{max-corrected} = \%P_{max-observed} \times [1 + \alpha \times (T_{module} - 25^{\circ}\text{C})]$$

with temperature coefficient,  $\alpha$

del Cueto filtered out observations taken during hazy sky conditions consisting of primarily diffuse radiation in order to analyze PV performance under clear sky conditions or direct radiation (del Cueto, 2007). Our work did not include significant filtering or the application of data correction factors, but these are areas of potential further research. Instead, we focused on reporting power generation and electrical characteristics under the real-world conditions that the test modules experienced. PV modules under test appear in Table 2 below.

**Table 2: PV Modules under test**

Tech	Module	Pmax (W)	I <sub>sc</sub> (A)	I <sub>MP</sub> (A)	V <sub>oc</sub> (V)	V <sub>MP</sub> (V)	Fill Factor	Temp Coeff Pwr (%/°C)	Area (m <sup>2</sup> )	Efficiency
c-Si	STP160S-24/Ab-1	160	5.0	4.65	43.2	34.4	0.74	-0.48	1.2766	12.5%
a-Si	Kaneka G-SA060	60	1.19	0.9	92	67	0.55	NA	0.9504	6.3%
CIGS	GSE PN 33030-O	30	2.2	1.7	25	17.5	0.54	-0.5	0.3937	7.6%
CIGS	Solyndra SL-001-165	165	2.74	2.37	93.9	69.6	0.64	-0.24	1.9656	8.4%
a-Si	USO PVL-68	68	5.1	4.13	23.1	16.5	0.58	-0.0021	1.1225	6.1%



## Results

The results of our numerical analyses appear in Appendices 5 through 7 for a-Si, c-Si, and CIGS modules respectively. Each appendix consists of graphs plotting  $\%P_{\max}$ ,  $I_{sc}$ ,  $V_{oc}$  and FF against POA irradiance,  $\%P_{\max}$  against AOI,  $\%P_{\max}$  and FF against module temperature, and FF and  $\%P_{\max}$  over time intervals.

The IEC proposed rating standard calls for linear interpolations of  $I_{sc}$ ,  $V_{oc}$ ,  $V_{mp}$  and  $P_{\max}$  with respect to temperature and irradiance as well as a polynomial interpolation of  $P_{\max}$  to irradiance and the equation  $V(\text{POA Irr}) = v1 \times \ln(\text{POA Irr}) + v2$  to interpolate  $V_{oc}$  to irradiance. Table 3 (below) shows the equations that we found for fitting  $\%P_{\max}$  to irradiance.

**Table 3: Trends in power by PV material**

Module Material	$\%P_{\max}$	$R^2$
	Trendline	
a-Si	$0.0010I_{rr} - 0.0740$	0.986
CIGS	$-0.0000004I_{rr}^2 + 0.0012I_{rr} - 0.0187$	0.974
c-Si	$0.000898I_{rr} - 0.0138$	0.994

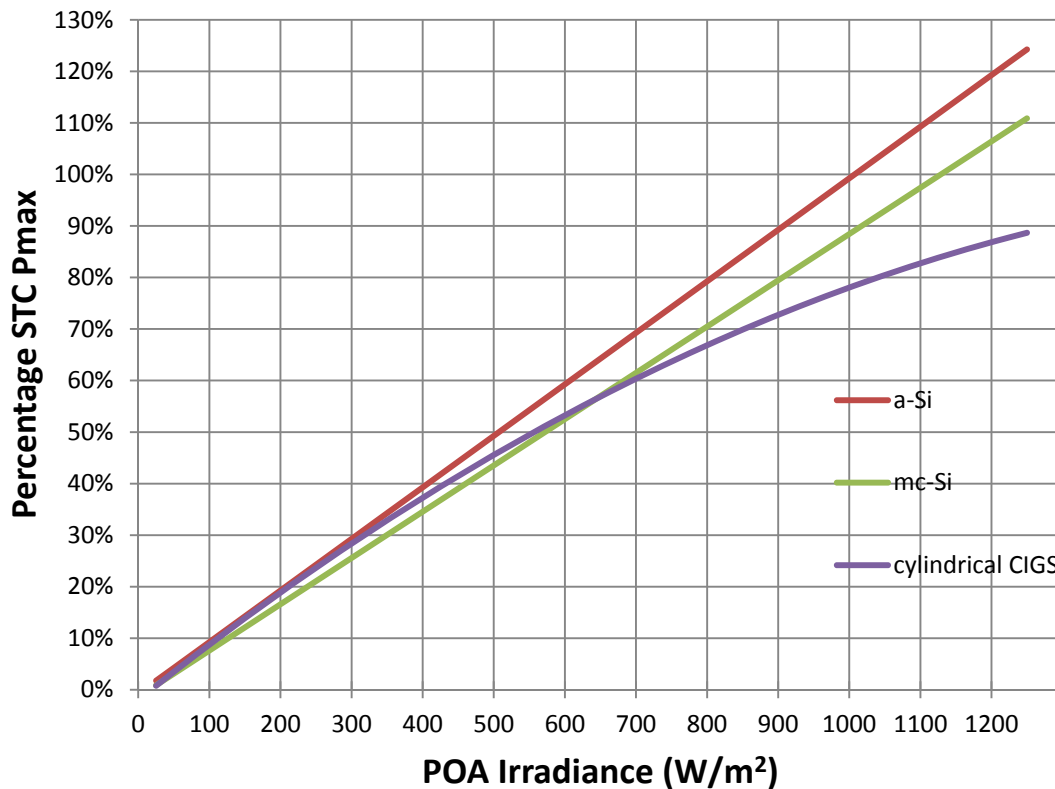
A linear relationship between power generation and irradiance clearly emerges in all cases (Appendices 5-7 a). A polynomial equation for CIGS provides a better fit than a linear equation, especially below  $1000\text{W}/\text{m}^2$ . As shown in Table 4 below, despite the strong linear relationship between power and irradiance, other factors (most notably, temperature and air mass) also affect power generation resulting in the following ranges of  $\%P_{\max}$  readings at full-sun ( $1000\text{W}/\text{m}^2$ ):

**Table 4: Power at 1000W/m<sup>2</sup> by PV material**

Module Material	%P <sub>max</sub> at Full-Sun (+/-0.5%)		
	Mean	Low	High
a-Si	101.1%	90.2%	106.1%
CIGS	78.9%	76.6%	86.0%
c-Si	86.2%	79.8%	94.1%

Inaccurate measurement devices and rapidly changing conditions during test periods also impact results.

As indicated in Figure 14 below, the a-Si module clearly demonstrates a superior power index to irradiance performance ratio. This corresponds to the equations presented in Table 3 above.

**Figure 14: Power vs POA Irradiance for a-Si, c-Si and CIGS modules**

a-Si modules deliver superior performance index results at higher levels of irradiance due to a favorable temperature coefficient. The manufacturers' state

temperature coefficients of  $-0.38\%/^{\circ}\text{C}$ ,  $-0.48\%/^{\circ}\text{C}$ , and  $-0.0021\%/^{\circ}\text{C}$  for their CIGS, c-Si and a-Si modules respectively.

For a-Si and c-Si, module temperatures typically average  $50\text{-}60^{\circ}\text{C}$  at full-sun. For c-Si, one can expect a  $50\text{-}60^{\circ}\text{C}$  module temperature to reduce  $P_{\text{max}}$   $12.5\text{-}17.5\%$  [ $(60-25) \times 0.48\%=17.5\%$ ] to a  $P_{\text{max}}$  between  $82.5\text{-}87.5\%$  of STC. This is consistent with our results.

Correcting for temperature on the c-Si module, a linear fit of  $P_{\text{maxcorr}} = 0.00106 \times \text{POA Irr} - 0.0582$  ( $R^2=0.976$ ) yields  $100.2\%$   $P_{\text{max}}$  at  $1000\text{W}/\text{m}^2$ . A polynomial fit of  $P_{\text{maxcorr}} = 0.00000012 \text{ POA Irr}^2 + 0.00118 \text{ POA Irr} - 0.711$  yields  $98.9\%$   $P_{\text{max}}$  at  $1000\text{W}/\text{m}^2$ .

Temperature-corrected observations and their corresponding linear and polynomial fits appear in Figure 15. This implies that at high irradiance conditions, when AM typically ranges between 1 and 2, AM does not significantly impact power generation. However, AM can exceed 10 near dawn and dusk and has a much greater influence over power under those, but not all low irradiance conditions.

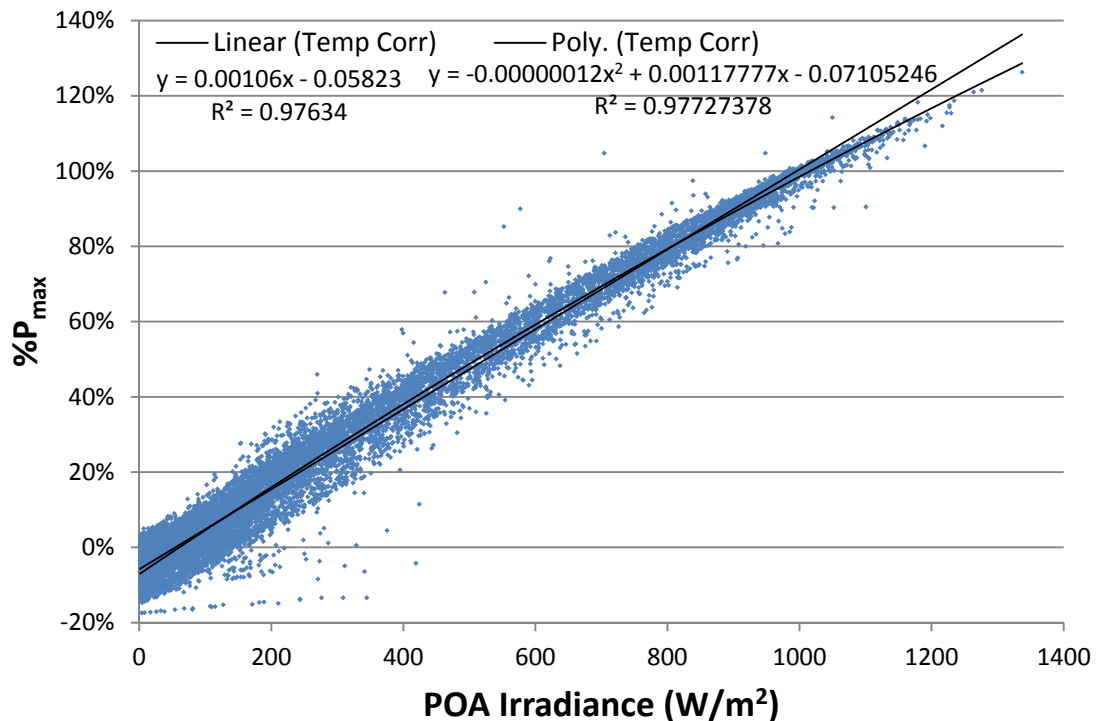


**Figure 15: Temperature corrected  $P_{\text{max}}$  c-Si**

Because the USO test-bed lacks the ability to measure AM and because there may be inaccuracies in its measurements of module temperature, our ability to measure and isolate temperature dependence is limited. However, having captured both nearby ambient and back of module temperatures along with power generation, POA irradiance and wind speed, we were able observe performance under a variety of real-world

conditions. Similar to Myers findings, observations from our study, presented in Appendix 8 indicate that wind speed does not strongly impact power (Myers, 2009).

Also as expected for a-Si, we see an oscillation in fill factors (i.e., efficiency) throughout the seasons from approximately 0.60 in mid-July to 0.53 in late December (Appendix 5 c). In terms of module temperature, FF ranges from 0.53 near 0°C to 0.60 between 30 and 50°C (Appendix 5 h). The downward trend from summer to winter is the result of an increased Staebler-Wronski effect under low temperature conditions and thermal annealing during warm periods (Gregg, Blieden, Chang, & Ng, 2005). c-Si and CIGS module FFs, on the other hand, remain steadier during the test period at 0.70 and 0.64, respectively (Appendices 6 and 7 c). The manufacturers list FFs of 0.74, 0.64, and 0.55 for c-Si, CIGS and a-Si, respectively.

In Appendices 5 through 7 b, the upper-band of observations up to 105° AOI represents clear sky conditions whereas the lower mass of observations reflect measurements taken under overcast conditions. Outliers above the band most likely indicate mostly sunny conditions with scattered clouds enhancing power through diffuse irradiance that enhances overall irradiance without obstructing direct sunlight. In these extreme cases, total POA irradiance exceeds full-sun (POA IRR>1000W/m<sup>2</sup>). This work did not include separating clear sky observations from cloudy skies, but del Cueto measured a specific PV module's performance under clear sky conditions with POA Irradiance = A + B x cos(AOI) and found:

<b>A</b>	<b>B</b>	<b>1 standard deviation</b>
- 87.4 ± 7.8 W/m <sup>2</sup>	1142.5 ± 20.9 W/m <sup>2</sup>	93.7 ± 11.2W/m <sup>2</sup>

He did this by fitting its photo-response as a function of AOI into segments (<=50, and 5° widths from 50-100° (del Cueto, 2007).

Our CIGS modules demonstrated increasing FF over a full range of increasing irradiance, as opposed a-Si and c-Si where FF decreases as irradiance increases beyond 500W/m<sup>2</sup>. (Refer to Appendices 5-7 d). This behavior indicates series-resistance.

a-Si, c-Si and CIGS modules exhibited an expected logarithmic relationship between V<sub>oc</sub> and irradiance. (Appendices 5-7 f) From existing literature, we know that CdTe also exhibit similar V<sub>oc</sub>, I<sub>sc</sub> and FF versus irradiance relationships as c-Si modules with approximately half the temperature coefficient (del Cueto, 2007).

Table 5 reports observations corresponding to the proposed IEC standard 61853-1 (+/- 50W/m<sup>2</sup> and +/-2.5°C). Note that relatively few measurements fit the standard's HTC and STC irradiance and temperature parameters.

**Table 5: United Solar Ovonic's Test-bed PV Power (W) Observations fitting IEC 61853-1 parameters**

		a-Si	c-Si	CIGS
HTC*	%P <sub>max</sub>	0.999	0.821	0.709
	Avg	60	131.3	117
	Min	55.8	124.8	102.1
	Max	63.9	139.2	130.8
	Obs	17	47	30
STC	%P <sub>max</sub>	0.968	0.921	0.643
	Avg	58.1	147.4	106.0
	Min	53.1	138.7	86.3
	Max	63.2	160.9	127.2
	Obs	5	4	91
NOCT	%P <sub>max</sub>	0.766	0.72	0.632
	Avg	46.0	115.1	104.3
	Min	39.3	104.8	97.1
	Max	52.6	132.6	125.7
	Obs	95	82	63
LTC	%P <sub>max</sub>	0.408	0.507	0.455
	Avg	24.5	71.6	75.0
	Min	20.5	63.7	62.4
	Max	30.4	81.2	105.7
	Obs	24	20	122
LIC	%P <sub>max</sub>	0.185	0.157	0.195
	Avg	11.1	25.2	32.2
	Min	5.3	14.3	20.7
	Max	15.8	35.2	50.2
	Obs	191	195	360

\* The cool, humid condition at the Auburn Hills, Michigan test site did not yield High Temperature Conditions, so these HTC observations include results for module temperatures as low as 60°C, rather than the IEC proposed standard of 75°C.

## Conclusion

The outdoor PV module testing system developed by United Solar Ovonic dramatically increased the organization's capabilities to test the performance of its competitors' and its own PV modules including prototypes. USO also relies on Spire simulators, accelerated testing and other means of testing PV in order to better understand and ultimately facilitate the advancement of PV technology.

The USO test-bed is effective at testing PV modules with  $I_{sc} < 6.4A$  (8/1.25 safety factor) and our results were consistent with both existing literature and the manufacturers' stated ratings. However, the array is located in a temperate-cool and humid region. Therefore, we were unable to generate a significant number of readings exhibiting the IEC's high temperature conditions (HTC). When compiling the observations reported in Table 4, we adjusted the module temperature parameter for HTC to include all measurements taken when module temperature exceeded 60°C, up to 15°C short of the HTC 75°C.

Irradiance produces power, but is expensive and difficult to measure precisely. In order to reduce uncertainty and to improve the accuracy of any PV measurement system, system operators should maintain properly calibrated secondary standard or first class pyranometers (Previtali, 2011). Other factors, most notably module temperature and air mass also affect power generation. Based on both our observations and manufacturers' claims, module temperatures under high temperature conditions can reduce  $P_{max}$  by 25%. True air mass is also difficult to measure and can affect power +/-8% under ordinary conditions (Kenny, Ioannides, Mullejans, & Dunlop, 2004).

Numerous opportunities exist for further research based on data generated by the test-bed. Our results support, but do not confirm the hypothesis that a-Si modules deliver more energy (kWhrs) per peak-watt ( $W_p$ ) than other PV materials. Confirming the hypothesis would require both testing a statistically significant number of PV modules and performing a quantitative analysis of the accuracy of the test-bed. The test-bed accommodates and tests 20 PV modules. USO has analyzed the performance of all of the modules under test, but this work compared the results of only three modules. Most of the other modules under test are USO current and next-generation a-Si. Better understanding of both the accuracy of the test-bed and the performance characteristics of a-Si could be attained by comparing measurements taken from the other modules under test.

Data filtering provides another avenue for further study. Separating clear sky readings from overcast sky readings is required in order to fit AOI effects.



Researchers analyze the constituent parameters of PV power, but developers and consumers understandably only care about power generation. The modules in this study produced between 0.76 and 0.95 W per kWh of POA irradiance per STC  $W P_{max}$ . These results appear in Appendix 9.

The modules under test produced between 51.5 and 105.1 dcW per kWh of POA irradiance per  $m^2$ . Given that PV modules are sold on a  $\$/W_p$  basis, efficiency becomes a secondary factor when selecting a module. However, efficiency quickly comes back into play as system developers and buyers consider space constraints (i.e., “roof rent”) and balance of system costs. 1000 square meters of array will require approximately the same amount of racking, wire, overcurrent protection, labor costs, etc. regardless of the technology and efficiency of the modules. In this case, a system with a higher efficiency module will generate more energy in the same amount of space as a less efficient panel and though the modules would have cost more based on their STC ratings, module cost represents only a fraction of the overall system cost. The balance of systems are likely to cost approximately the same amount regardless of the PV module material. For these reasons PV module efficiency remains an important factor for consideration.

## Glossary

$\eta$	Efficiency with respect to reference conditions
$\lambda$	Wavelength
$A$	Test module area
$\alpha$ -Si	Amorphous Silicon
$AM$	Air Mass
$AOI$	Angle of Incidence
$c$ -Si	Crystalline Silicon
$CIGS$	Copper Indium Galium Selenide
<i>Energy yield</i>	Whrs/ $W_p$
$E_{ref}(\lambda)$	Reference spectral irradiance
$E_s(\lambda)$	Measured spectral irradiance of the light source
$E_t$	Total irradiance
$FF$	Fill factor
$I_{mp}$	Current at $P_{max}$
$I_{sc}$	Test module short-circuit current
$IEC$	International Electrotechnical Commission
<i>Inverter ramp-times</i>	AC power losses that occur during sudden fluctuations in irradiance
<i>Inverter clipping</i>	AC power losses that occur when array power exceeds inverter capability
$IRR$	Calibrated current of the reference cell under the reference conditions
$ITM$	Measured test cell current
$ITR$	Calibrated current of the test cell under the reference conditions
$I-V$	Current versus voltage
$K$	Spectral correction factor, inverse of $M$
$M$	Spectral mismatch parameter
$P_{max}$	Test module maximum power under reference conditions
$POA$	Plane of Array
$St(\lambda)$	Measured spectral responsivity of the test module

$S_r(\lambda)$	Measured spectral responsivity of the reference module
$STC$	Standard Test Conditions ( $1000\text{W}/\text{m}^2$ , $25^\circ\text{C}$ mod temp, 1.5 AM)
$V_{mp}$	Test module voltage at $P_{max}$
$V_{oc}$	Test module open-circuit voltage

## References

- Device Performance. (2006, June). *Measurement and Characterization - National Center for Photovoltaics*. Golden, CO: National Renewable Energy Laboratory.
- Enphase Energy. (2011). Retrieved July 15, 2011, from <http://enphase.com/products/enlighten/>
- Fronius USA LLC. (2011). Retrieved July 15, 2011, from [http://www.fronius.com/cps/rde/xchg/SID-523BEC85-1CC3FCC9/fronius\\_usa/hs.xsl/2714\\_1458.htm](http://www.fronius.com/cps/rde/xchg/SID-523BEC85-1CC3FCC9/fronius_usa/hs.xsl/2714_1458.htm)
- Keithley Instruments. (2011). Retrieved July 15, 2011, from <http://www.keithley.com/rpCMSimg/50675>.
- del Cueto, J. A. (2007). *PV Module Energy Ratings Part II: Feasibility of Using the PERT in Deriving Photovoltaic Module Energy Ratings*. Golden, CO: National Renewable Energy Laboratory.
- Dierauf, T. (2011, May 20). SunPower Energy Management Services ASES Solar 2011. Raleigh, NC.
- Emery, K. (2009). *Uncertainty Analysis of Certified Photovoltaic Measurements at the National Renewable Energy Laboratory*. Golden, CO: National Renewable Energy Laboratory.
- Emery, K. A., Osterwald, C. R., Cannon, T. W., Myers, D. R., Burdick, J., Glatfelter, T., et al. (1985). Methods for Measuring Solar Cell Efficiency Independent of Reference Cell or Light Source. *18th Photovoltaic Solar Conference* (pp. 623-628). Las Vegas, NV: Institute for Electrical and Electronic Engineers.
- Emery, K., Anderberg, A., Kiehl, J., Mack, C., Moriarty, T., Rummel, S., et al. (2005). Trust But Verify: Procedures to Achieve Accurate Efficiency Measurements for All Photovoltaic Technologies. *31st IEEE Photovoltaic Specialists Conference and Exhibition* (pp. 1-5). Lake Buena Vista, FL: Institute of Electrical and Electronic Engineers.
- Emery, K., DelCueto, J., & Zaيمان, W. (2003). Spectral Corrections Based on Optical Air Mass. *Photovoltaic Specialists Conference, 2002. Conference Record of the Twenty-Ninth IEEE* (pp. 1725-1728). New Orleans, LA: IEEE.
- Gay, C. F., Rumberg, J. E., & Wilson, J. H. (1982). AM-PM: all day module performance measurements. *Proceedings 16th IEEE Photovoltaic Specialist' Conference* (pp. 1041-1046). San Diego, CA: IEEE.
- Gregg, A., Blieden, R., Chang, A., & Ng, H. (2005). Performance Analysis of Large Scale, Amorphous Silicon Photovoltaic Power Systems. *31st Photovoltaic Specialist Conference and Exhibition*. Lake Buena Vista, FL: Institute of Electrical and Electronics Engineers.

- Gregg, A., Parker, T., & Swenson, R. (2005). A "Real World" Examination of PV Systems Design and Performance. *31st Photovoltaic Specialist Conference and Exhibition*. Lake Buena Vista, FL: Institute of Electrical and Electronics Engineers.
- Jansen, K. W., Kadam, S. B., & Groelinger, J. F. (2006). The High Energy of Amorphous Silicon Modules in a Hot Coastal Climate. *21st European Photovoltaic Solar Energy Conference*, (pp. 2535-2538). Dresden (Germany).
- Kenny, R. P., Dunlop, E. D., Ossenbrink, H. A., & Mullejans, H. (2006, December 19). A Practical Method for the Energy Rating of c-Si Photovoltaic Modules Based on Standard Tests. *Progress in Photovoltaics: Research and Applications*, 14:155-166.
- Kenny, R. P., Ioannides, A., Mullejans, H., & Dunlop, E. D. (2004). Spectral effects on the energy rating of thin film modules. *Proceedings of the 19th EUPVSEC*, (pp. 2451-2454). Paris, France.
- Kimber, A. (2011, May 20). PV System Capacity Testing: Methods, Constraints and Applications. Raleigh, NC.
- King, D. L., Kratochvil, J. A., & Boyson, W. E. (1997). Measuring Solar Spectral and Angle-of-Incidence Effects on Photovoltaic Modules and Solar Irradiance Sensors. *26th IEEE Photovoltaics Specialists Conference* (pp. 1-6). Anaheim, CA: Sandia National Laboratories.
- Marion, B. (2000). Validation of a Photovoltaic Module Energy Ratings Procedure at NREL. *NCPV Program Review Meeting* (pp. 85-86). Denver, CO: NREL.
- Marion, B., Kroposki, B., Emery, K., del Cueto, J., Myers, D., & Osterwald, C. (1999). *Validation of a Photovoltaic Module Energy Ratings Procedure at NREL*. Golden, CO: National Renewable Energy Laboratory.
- Myers, D. (2009). Evaluation of the Performance of the PVUSA Rating Methodology Applied to Dual Junction PV Technology. *American Solar Energy Society Annual Conference* (pp. 1-11). Buffalo, NY: National Renewable Energy Laboratory.
- Poissant, Y., Pelland, S., & Turcotte, D. (2008). A COMPARISON OF ENERGY RATING METHODOLOGIES USING FIELD TEST MEASUREMENTS. *23rd European PV Solar Energy Conference and Exhibition* (pp. 1-6). Valencia, Spain: CANMET Energy Technology Center.
- Previtali, J. (2011, May 20). An Independent Engineer's views on PV Performance Testing. Raleigh, NC.
- Reda, I., & Andreas, A. (2008). *Solar Position Algorithm for Solar Radiation Applications*. Golden, CO: National Renewable Energy Laboratory.

Riordan, C., & Hulstron, R. (1990). What is an Air Mass 1.5 Spectrum? *Conference Record of the Twenty First IEEE* (pp. 1085-1088). Kissimmee, FL: Photovoltaic Specialists Conference.

van Cleef, M., Lippens, P., & Call, J. (2001). Superior Energy Yields of UNI-SOLAR Triple Junction Thin Film Silicon Solar Cells compared to Crystalline Silicon Solar Cells under Real Outdoor Conditions in Western Europe. *17th European Photovoltaic Solar Energy Conference and Exhibition*. Munich (Germany).

**Appendices**

Appendix 1: Measurement Device Data Sheets ..... 28  
 Appendix 2: Comparison of pyranometer readings ..... 32  
 Appendix 3: System Design..... 33  
 Appendix 4: Module Data Sheets ..... 36  
 Appendix 5: a-Si module Results ..... 42  
 Appendix 6: c-Si module Results..... 47

Graph	Axis	
	x	y
a	POA Irr W/m <sup>2</sup>	%P <sub>max</sub>
b	AOI	%P <sub>max</sub>
c	Date	Fill Factor
d	POA Irr W/m <sup>2</sup>	Fill Factor
e	POA Irr W/m <sup>3</sup>	I <sub>sc</sub>
f	POA Irr W/m <sup>4</sup>	V <sub>oc</sub>
g	Module Temp °C	%P <sub>max</sub>
h	Module Temp °C	Fill Factor
i	Date	%P <sub>max</sub>

Appendix 7: CIGS module Results..... 52

Graph	Axis	
	x	y
a	POA Irr W/m <sup>2</sup>	%P <sub>max</sub>
b	AOI	%P <sub>max</sub>
c	Date	Fill Factor
d	POA Irr W/m <sup>2</sup>	Fill Factor
e	POA Irr W/m <sup>3</sup>	I <sub>sc</sub>
f	POA Irr W/m <sup>4</sup>	V <sub>oc</sub>
g	Ambient Temp °C	%P <sub>max</sub>
h	Ambient Temp °C	Fill Factor
i	Date	%P <sub>max</sub>

Appendix 8: Power versus wind speed c-Si module ..... 57

Appendix 9: Conclusions ..... 58

## Appendix 1: Measurement Device Data Sheets

## Kipp and Zonen SPLite2 Photodiode Pyranometer

**SP Lite2** is a simple pyranometer for routine measurements of solar radiation. It has a cosinelike diffuser that provides excellent directional (cosine) response, causes rain to run off and is easy to clean. Although the spectral range is limited by the photo-diode detector, the performance of the SP Lite2 compares favorably to ISO 9060 Second Class thermopile pyranometers under clear and unobstructed natural daylight conditions.

The mounting flange incorporates a bubble level and adjustment screws, for easy levelling. A threaded hole takes the accessory screw-in mounting rod for fitting to masts and poles. Two SP Lite2 instruments can easily be bolted back-to-back, and fitted with the mounting rod, to make a simple albedometer. The standard cable length is 5 m, with an option of 15 m. SP Lite2 is ideal for use with the METEON handheld display and data logger for field test use.

## Specifications

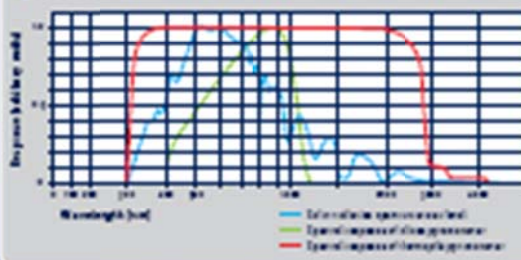
Response time (95%)	< 500 ms
Non-stability (change/year)	< 2%
Non-linearity (0 to 1000 W/m <sup>2</sup> )	< 1%
Directional error (up to 80° with 3000 W/m <sup>2</sup> beam)	< 5 W/m <sup>2</sup>
Temperature dependence (-30 °C to +70 °C)	- 0.25%/°C

## Other specifications

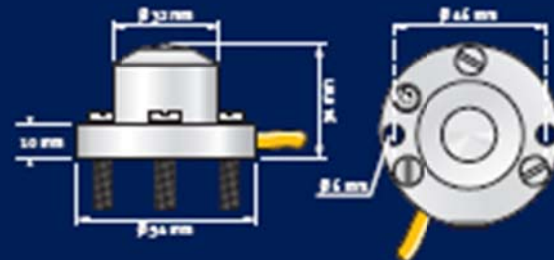
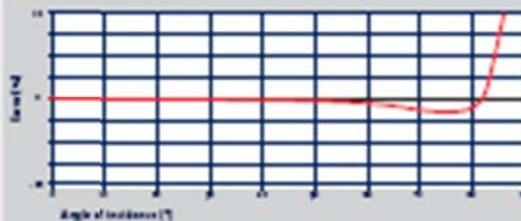
Sensitivity	60 to 100 µV/(W/m <sup>2</sup> )
Impedance	50 Ω
Operating temperature	-30 °C to +70 °C
Spectral range	300 to 1300 nm
Typical signal output for atmospheric applications	0 to 100 mV
Maximum irradiance	2000 W/m <sup>2</sup>
Detector	Silicon photo-diode

SP Lite2 has a standard coptive cable of 5 m length. Optional cable length 15 m.

## Spectral response



## Directional response



## Albedo set-up



## Optional mounting rod





### Kipp and Zonen CMP-21 Secondary Standard Thermopile Pyranometer



Specifications	CMP-21
ISO Classification	Secondary Standard
Response time (95%)	< 5 s
<u>Zero offsets</u>	
(a) thermal radiation (200W/m <sup>2</sup> )	< 3 W/m <sup>2</sup>
(b) temperature change (5 K/hr)	< 1 W/m <sup>2</sup>
Non-stability (change/year)	< 0.5%
Non-linearity (0 to 1000 W/m <sup>2</sup> )	< 0.2%
Directional error (up to 80° with 1000W/m <sup>2</sup> beam)	< 5 W/m <sup>2</sup>
Temperature dependence of sensitivity	< 0.5% (-20 °C to +50 °C)
Tilt error (at 1000 W/m <sup>2</sup> )	< 0.2%
Sensitivity	< 7 to 14 μV/W/m <sup>2</sup>
Impedance	10 to 100 Ω
Level accuracy	0.1 °
Operating temperature	-40 °C to +80 °C
Spectral range (50% points)	285 to 2800 nm
Typical signal output for atmospheric applications	0 to 15 mV
Maximum irradiance	< 4000 W/m <sup>2</sup>
Expected daily uncertainty	< 1%
Recommended applications	Meteorological networks, reference measurements in extreme climates

## Keithley Instruments Model #2700 Data Acquisition System

## Condensed specifications\*

**DC VOLTAGE**

1000V protection in all ranges; AD Linearity of 1ppm/rdg + 1ppm/rng; 120000 max counts

Range	Reso- lution	Accuracy (90 day rdg + rng)	Accuracy (1 year rdg + rng)	Input Resistance
330.0000mV	330nV	0.0325% + 0.0125%	0.0593% + 0.0075%	10M $\Omega$ or > 10GD
1.000000V	1.0 $\mu$ V	0.0325% + 0.0125%	0.0593% + 0.0075%	10M $\Omega$ or > 10GD
10.00000V	10 $\mu$ V	0.0320% + 0.0125%	0.0593% + 0.0075%	10M $\Omega$ or > 10GD
100.0000V	100 $\mu$ V	0.0325% + 0.0125%	0.0593% + 0.0075%	10M $\Omega$
1000.000V	1mV	0.0325% + 0.0125%	0.0593% + 0.0075%	10M $\Omega$

**THERMOCOUPLE**

Conversion to IEC43, Automatic, Internal, or Standardized CJC, Open C/C check.

Type	Range	Accuracy (1 year with standardized CJC)	Accuracy (1 year with automatic CJC)
J	-20 to +360°C	$\pm 0.2^\circ\text{C}$ for all ranges	$\pm 1.0^\circ\text{C}$
K	-20 to +1572°C	$\pm 0.2^\circ\text{C}$ for all ranges	$\pm 1.0^\circ\text{C}$
N	-20 to +150°C	$\pm 0.2^\circ\text{C}$ for all ranges	$\pm 1.0^\circ\text{C}$
T	-20 to +400°C	$\pm 0.2^\circ\text{C}$ for all ranges	$\pm 1.0^\circ\text{C}$
E	-20 to +1000°C	$\pm 0.2^\circ\text{C}$ for all ranges	$\pm 1.0^\circ\text{C}$
R	0 to +3760°C	$\pm 0.6^\circ\text{C}$ for all ranges	$\pm 1.8^\circ\text{C}$
S	0 to +3760°C	$\pm 0.6^\circ\text{C}$ for all ranges	$\pm 1.8^\circ\text{C}$
B	-450 to +3820°C	$\pm 0.6^\circ\text{C}$ for all ranges	$\pm 1.8^\circ\text{C}$

**RESISTANCE**

3- or 4-wire, Offset Compensation selectable; 1000V / 550V protection on source / sense inputs

Range	Reso- lution	Accuracy (90 day rdg + rng)	Accuracy (1 year rdg + rng)	Max Current
100.0000 $\Omega$	10 $\mu\Omega$	0.0080% + 0.0030%	0.0333% + 0.0030%	1mA
1.000000 $\Omega$	1.0n $\Omega$	0.0080% + 0.0030%	0.0333% + 0.0030%	1mA
10.00000 $\Omega$	10n $\Omega$	0.0080% + 0.0030%	0.0333% + 0.0030%	100 $\mu$ A
100.0000 $\Omega$	100n $\Omega$	0.0080% + 0.0030%	0.0333% + 0.0030%	10 $\mu$ A
1.000000k $\Omega$	1.0 $\Omega$	0.0080% + 0.0030%	0.0333% + 0.0030%	10 $\mu$ A
10.00000k $\Omega$	10 $\Omega$	0.0200% + 0.0030%	0.0400% + 0.0030%	0.7 $\mu$ A
100.0000k $\Omega$	100 $\Omega$	0.2000% + 0.0030%	0.1500% + 0.0030%	0.7 $\mu$ A

**RTD**

D100, F100, F230, F2500, or user type, plus probe error

Range	Resolution	Accuracy (1 year)
-200 to +900°C	0.001°C	$\pm 0.05^\circ\text{C}$

**THERMISTOR**1.5k $\Omega$ , 5k $\Omega$ , and 10k $\Omega$  plus sensor error

Range	Resolution	Accuracy (1 year)
-200 to +900°C	0.001°C	$\pm 0.05^\circ\text{C}$

**DC CURRENT**

250V, 5A fused inputs, Built-in shunt resistors

Range	Reso- lution	Accuracy (90 day rdg + rng)	Accuracy (1 year rdg + rng)	Input Resistance
33.00000mA	330nA	0.02% + 0.014%	0.05% + 0.004%	< 0.2V
330.0000mA	330nA	0.02% + 0.014%	0.05% + 0.004%	< 0.05V
1.00000A	1 $\mu$ A	0.02% + 0.014%	0.05% + 0.004%	< 0.5V
3.00000A	10 $\mu$ A	0.12% + 0.014%	0.12% + 0.004%	< 1.0V

**AC VOLTAGE**

True RMS, 5.1 max Crest Factor

Range	Resolution	Frequency Range	Accuracy (1 year rdg + rng)
33mV to 750V	0.1 $\mu$ V to 1mV	5Hz - 10kHz	0.3% + 0.05%
		30Hz - 20kHz	0.05% + 0.05%
		20kHz - 50kHz	0.12% + 0.05%
		50kHz - 100kHz	1.6% + 0.06%
		100kHz - 200kHz	4.0% + 0.5%

**FREQUENCY and PERIOD**

Selectable Gate Times of 10ms, 100ms, 1sec

Range	Frequency Range	Period Range	Accuracy (1 year rdg + rng)
33mV to 750V	5Hz to 500kHz	55ns to 0.2sec	0.01% + 0.55ppm (1.0 sec) 0.01% + 0.55ppm (0.1 sec) 0.01% + 1.55ppm (0.01 sec)

**AC CURRENT**

True RMS, 5.1 Crest Factor

Range	Resolution	Frequency Range	Accuracy (1 year rdg + rng)
1A	1 $\mu$ A	10Hz - 50Hz	0.25% + 0.05%
5A	10 $\mu$ A	10Hz - 50Hz	0.15% + 0.05%

**DC READING RATES**

Function	Digits	Readings/sec	NPLC
DCV DCL	6.5	5	33
2W Ohms	6.5	50	1
	5.5	250	0.1
	4.5	200	0.01
4W Ohms, RTD	6.5	2.5	33
Thermistor	6.5	25	1
Thermocouple	5.5	125	0.1
	4.5	250	0.01

**DC READING SPEED VS. NOISE REJECTION**

NPLC	Digits	Filter	NOISE	CMRR	EMF Noise (10V range)
10	6.5	50	110dB	140dB	< 1.2 $\mu$ V
1	6.5	OFF	90dB	140dB	< 4.0 $\mu$ V
0.1	5.5	OFF	-	93dB	< 22 $\mu$ V
0.01	4.5	OFF	-	93dB	< 150 $\mu$ V

**SCANNING RATE, INTO AND OUT OF MEMORY TO GPIB**

Function	Channels/s
7700 scanning DCV	25/s
7700 scanning DCV with limits or timestamp on	15/s
7700 scanning DCV alternating 2W	6/s
7702 scanning DCV	6/s
7700, 7706, and 7708 scanning temperature (T/C)	5/s

**SYSTEM FEATURES**

Scanning Channels	Up to 80 differential
Trigger Source	Internal digital input, front panel keypad, channel monitor, internal timer, GPIB 25-252, Trigger link, immediate
Scan Counts	1 to 50,000 or continuous
Scan Interval	0 to 99 hours, linear step size
Channel Delay	0 to 999999sec per channel, linear step size
Configuration	Per channel for measurement setup, math, and limits
Power Fail Recovery	Resume scanning sequence, configuration and stored data are preserved
Power up Memory	4 user configurations with labels
Real Time Clock	Included, use to timestamp readings
Data Storage	Non-volatile 55,000 reading buffer with timestamp, continuous file query while filing, min/max/avg/hd dev
Alarm Limits	2 HI and 2 LO limits per channel, selectable polarity
Digital Input	2 TTL level - external trigger plus interlock
Digital Output	4 TTL level - selectable polarity, HILLO limit configurable
Master Alarm	1 TTL level output toggles when any HILLO limit is exceeded
Front Panel Lock	Software enabled
Communication	IEEE-488.2, RS-232
Per-channel Math	mZ + b, R
Multi-channel Math	Ratio, Average
Resolution	6+ digit with 20% overrange, 28-bit readings available over IEEE-488
Software	Unix/PC-based main-up applications, LabVIEW, WinPoint, IntWindows/CVI, Visual Basic, C/C++ driver

**GENERAL INFORMATION**

Power Supply	100V / 120V / 220V / 240V / $\pm 10\%$
Line Frequency	45Hz to 60Hz, 50Hz to 400Hz
Operating Environment	0°C to 50°C
Size	80mm H x 215mm W x 370mm D
Warranty	3 years on mainframe, 1 year on Measurements & Control Modules
Safety	UL 9113-1, IEC 3018-1, CSA
EMC	CE mark, FCC Class A

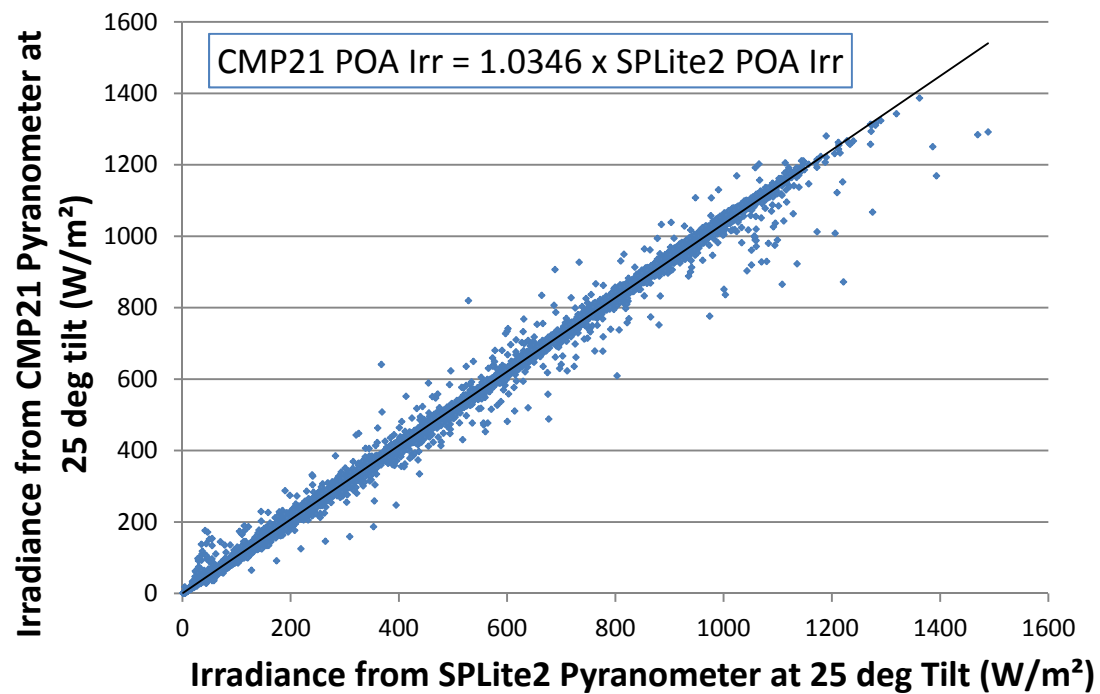
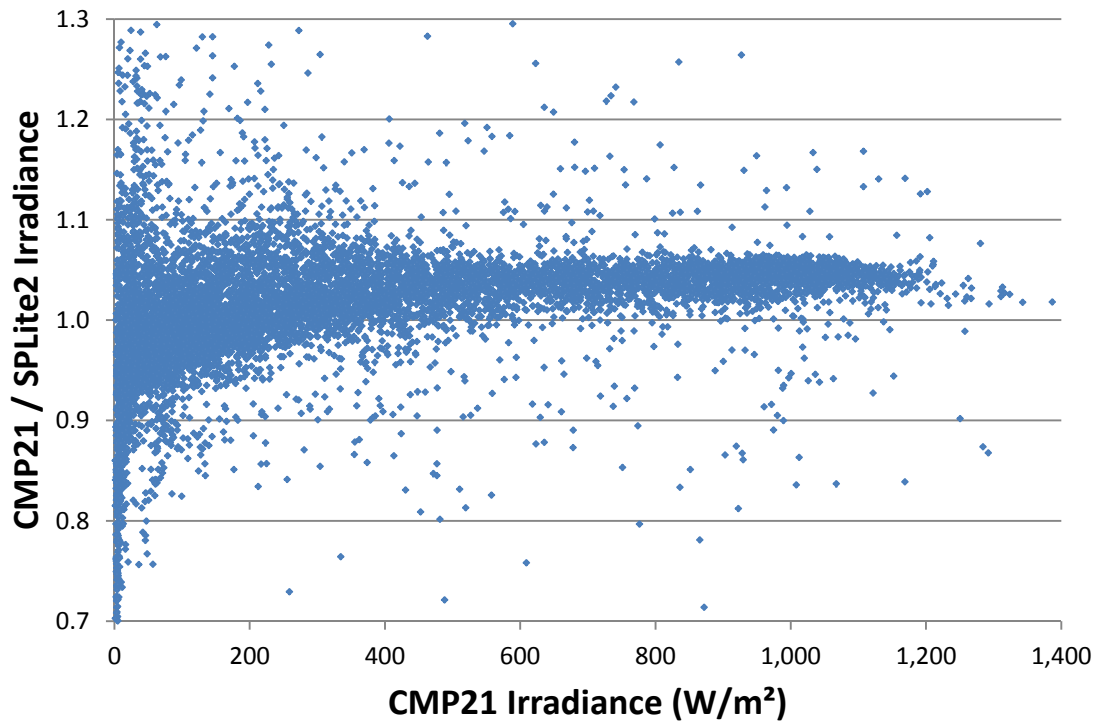
\* Visit [www.keithley.com](http://www.keithley.com) for detailed specifications.

Specifications subject to change without notice.

**KI 2430 Source Meter Specifications:**

Volts Ranges	0.2, 2, 20, 100V
Basic V Source Accuracy	0.02%
Basic V Measure Accuracy	0.015%
I Ranges	1, 10, 100 $\mu$ A
	1, 10, 100 mA
	1, 3, 10 A
Basic I Source Accuracy	0.045%
Basic I Measure Accuracy	0.035%
Ohms Ranges	2, 20, 200 $\Omega$
	2, 20, 200 k $\Omega$
	2, 20, 200 M $\Omega$
Basic Ohms Measure Accuracy	0.06%
Maximum Power	110 W DC
	1000W Pulse

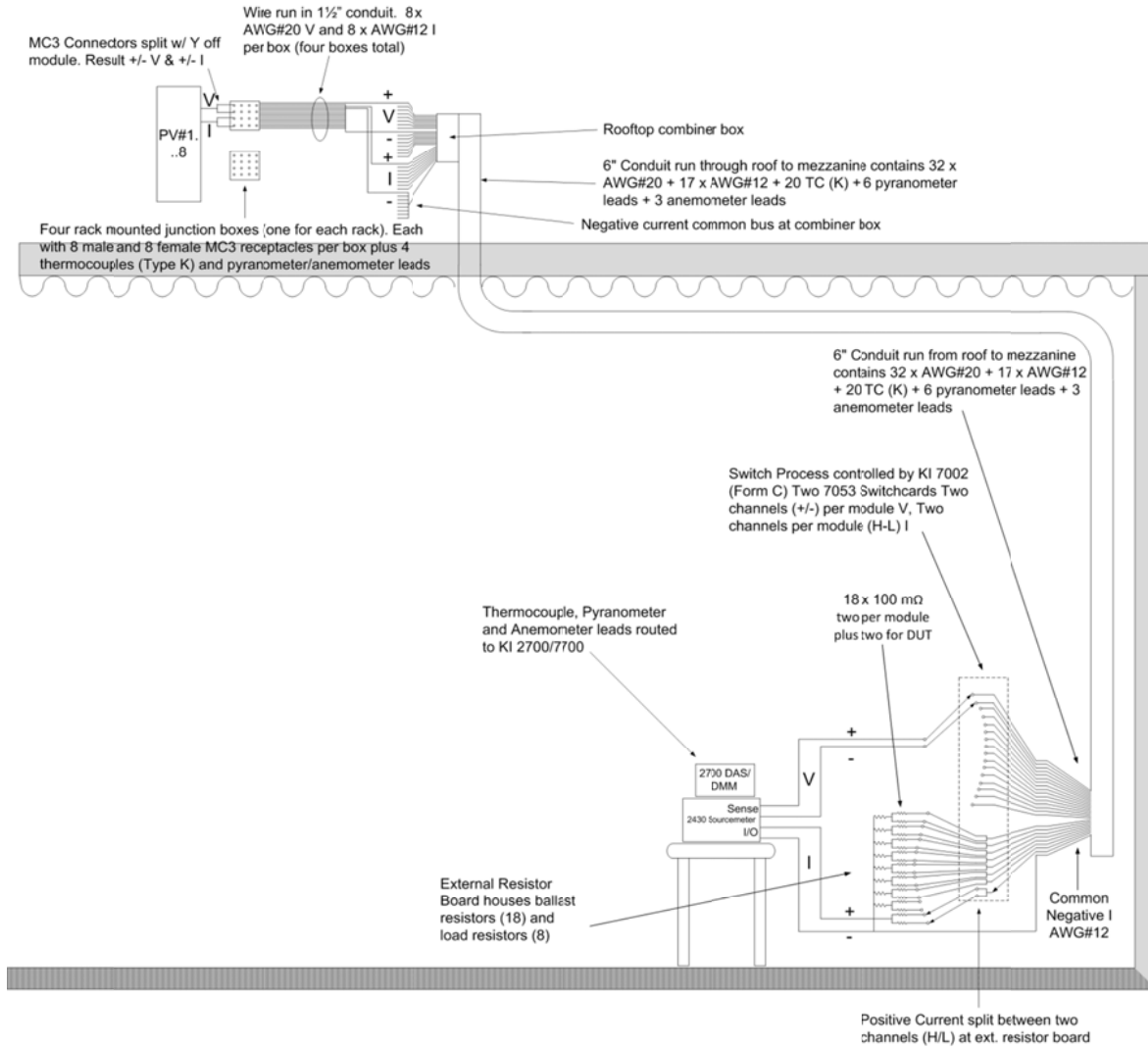
## Appendix 2: Comparison of pyranometer readings



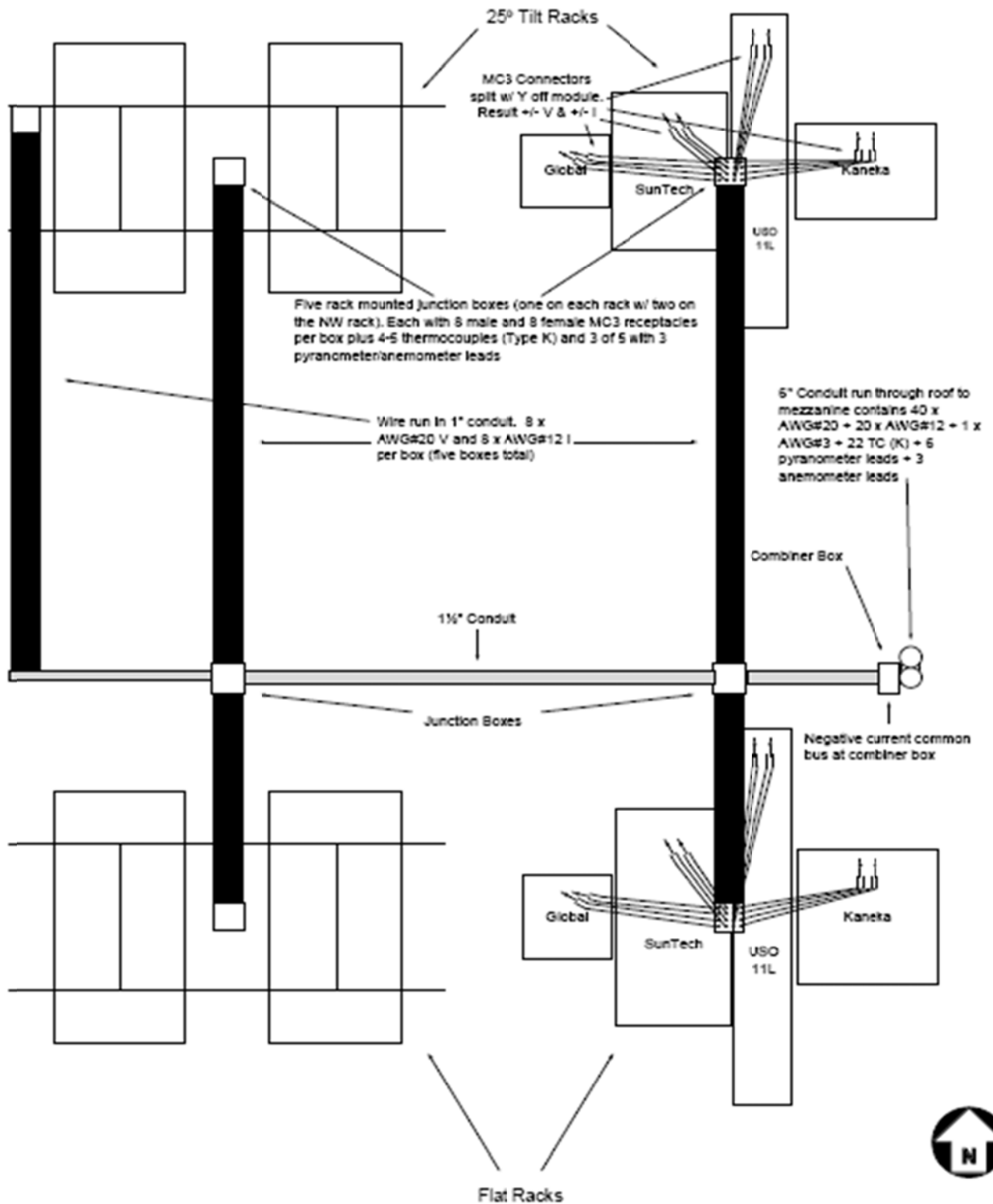
### Appendix 3: System Design

<b>System Components</b>
Keithley Instruments (KI) Source Meter #2430
KI Switching Mainframe #7002
Four KI Switching Modules #7053
<i>4A channels ( x 2 = 8A)</i>
<i>100mΩ H/L channel ballast resistors</i>
KI DMM Data Acquisition System #2700/7700
Kipp & Zonen CMP-21 thermopile pyranometer
Three Kipp & Zonen Pyranometers SP-Lite 2 (flat, 15°, and 27°)
Maximum Anemometer #41
Type (K) Thermocouples (each module and two ambient)
PC with GPIB interface
<i>VBA.net</i>
Fixed load resistors (Minimum Power Rating = $V_{mp}/I_{mp} \times 1.25$ )
Block-ballasted non-penetrating racks

### System Diagram



### Rooftop Schematic

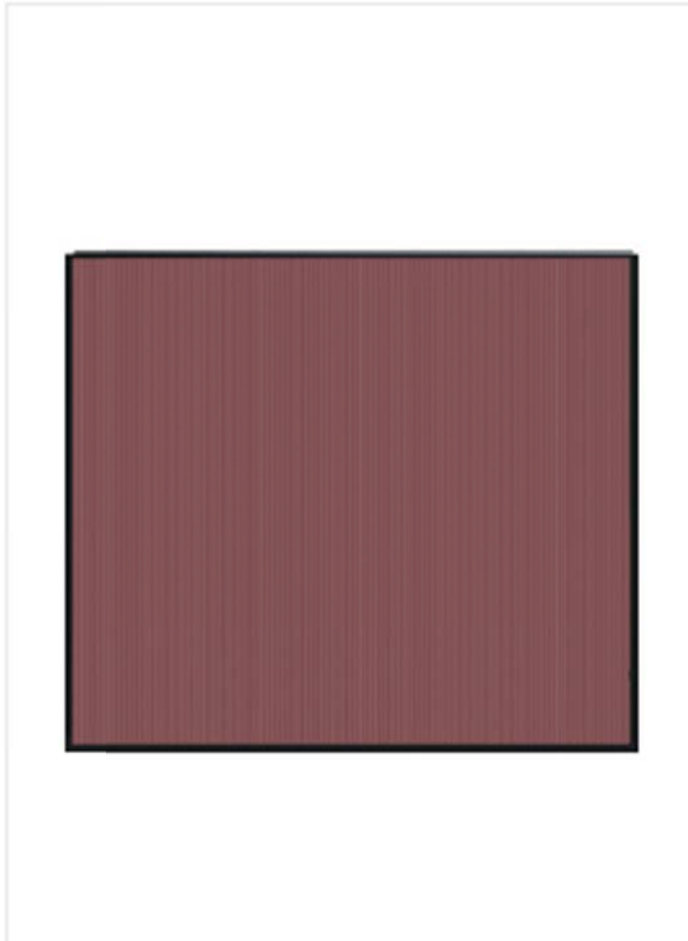


## Appendix 4: Module Data Sheets



### SOLAR MODULE Silicon Thin-film

Kaneka K60 same as GSA-60



#### Quality

- IEC 61646 tested and certified
- safety class II for 530 V system voltage (projected)

#### Guarantee

- 25 years power warranty (80%)\*
- 12 years power warranty (90%)\*
- 5 years product guarantee\*

#### High performance

- power tolerance +10%... -5%
- higher yield on plant due to higher power output on delivery
- high yields even at high module temperatures

#### Ecological advantage

- Extremely low consumption on material → energy payback time less than 2 years

#### Design

- Homogeneous colouring of frame and module surface → high-class, harmonic appearance

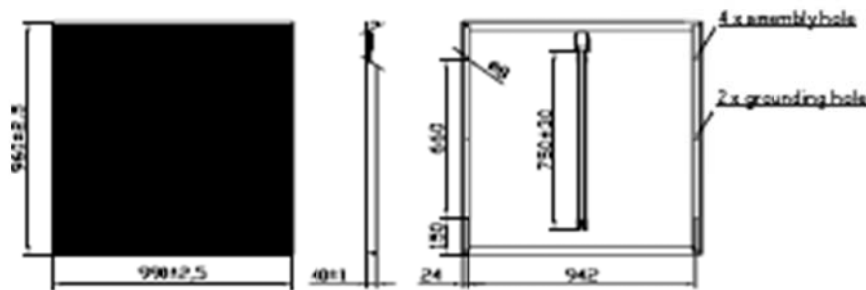




## Your advantages at a glance

- power tolerance +10%... -5%
- IEC 61646 tested and certified
- safety class II for system voltage up to 530 V (projected)
- power warranty 25 years (80%), 12 years (90%)\*
- product guarantee 5 years\*
- higher yield on plant due to higher power output on delivery
- high yields even at high module temperatures
- ecological advantage – extremely low consumption on material – energy payback time less than 2 years
- delivered ready for connection with cable and Multi-Contact plug-in connectors
- Integrated bypass diodes
- 100% end control

**Attention:**  
The laser lines have to be installed with at least 10° inclination. Please observe the installation instructions.



Electrical values under standard test conditions 1000 W/m<sup>2</sup>; 25°C; AM1,5.

Electrical power values +10 %... -5 %.  
Other electrical values ±10 %

(\*) The complete and individual valid guarantee conditions are relevant, which will be handed out by your IBC-representative on request.

Subject to modifications that represent progress.

## Technical data

		Stabilised values	Initial values
Nominal peak power	(Wp)	60,0	70,0
Guaranteed minimum power	(Wp)	57,0	75,06
Nominal voltage	(V)	67,0	74,0
Nominal current	(A)	0,90	1,04
Open-circuit voltage	(V)	92,0	96,0
Short-circuit current	(A)	1,19	1,22
Maximum system voltage	(V)		530
Length	(mm)		960
Width	(mm)		990
Height	(mm)		40
Weight	(kg)		14
Assembly holes ø 8 mm	(pieces)		4



Solar powering a green future™

STP175S - 24/Ab-1  
STP170S - 24/Ab-1  
STP165S - 24/Ab-1  
STP160S - 24/Ab-1

## 175 Watt

### MONO-CRYSTALLINE SOLAR PANEL

#### Features

- High conversion efficiency based on innovative photovoltaic technologies
- High reliability with guaranteed +/-3% power output tolerance
- Withstands high wind-pressure and snow load, and extreme temperature variations

#### Quality and Safety

- 25-year power output transferable warranty
- Rigorous quality control meeting the highest international standards
- ISO 9001:2000 (Quality Management System) and ISO 14001:2004 (Environmental Management System) certified factories manufacturing world class products
- UL listings: UL1703, cULus, Class C fire rating, conformity to CE

#### Recommended Applications

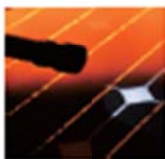
- Residential roof top systems
- On-grid utility systems
- On-grid commercial systems



Suntech's technology yields improvements to BSF structure and anti-reflective coating to increase conversion efficiency



Unique design on drainage holes and rigid construction prevents frame from deforming or breaking due to freezing weather and other forces



The panel provides more field power output through an advanced cell texturing and isolation process, which improves low irradiance performance



Suntech was named Frost and Sullivan's 2008 Solar Energy Development Company of the Year

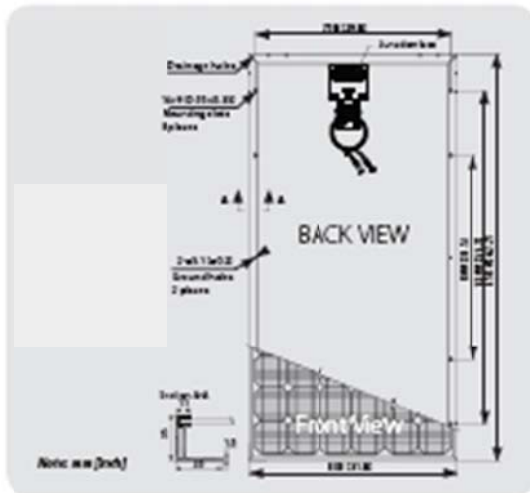


Solar powering a green future™

### Electrical Characteristics

Characteristics	STP180S-24/Ab-1	STP175S-24/Ab-1	STP170S-24/Ab-1	STP165S-24/Ab-1	STP160S-24/Ab-1
Open - Circuit Voltage (Voc)	44.4V	44.2V	43.8V	43.6V	43.2V
Optimum Operating Voltage (Vmp)	35.6V	35.2V	35.2V	34.8V	34.4V
Short - Circuit Current (Isc)	5.4A	5.2A	5.14A	5.04A	5A
Optimum Operating Current (Imp)	5.05A	4.95A	4.83A	4.74A	4.65A
Maximum Power at STC (Pmax)	180Wp	175Wp	170Wp	165Wp	160Wp
Operating Temperature	-40°C to +85°C	-40°C to +85°C	-40°C to +85°C	-40°C to +85°C	-40°C to +85°C
Maximum System Voltage	600V DC	600V DC	600V DC	600V DC	600V DC
Maximum Series Fuse Rating	15 AMPS	15 AMPS	15 AMPS	15 AMPS	15 AMPS
Power Tolerance	±3 %	±3 %	±3 %	±3 %	±3 %

STC: Irradiance 1000W/m<sup>2</sup>, Module temperature 25°C, AM:1.5



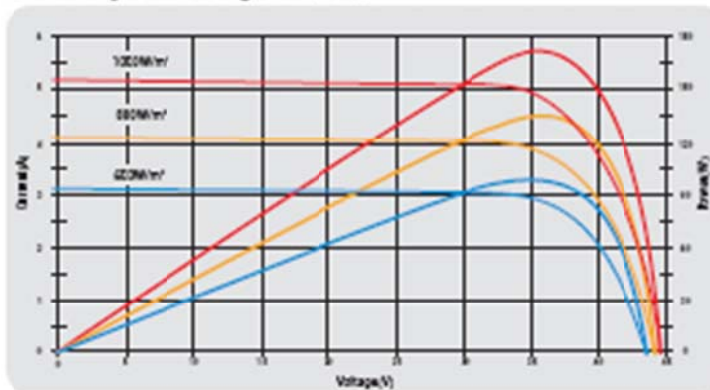
### Mechanical Characteristics

Solar Cell	Mono-crystalline 125x125mm (5inch)
No. of Cells	72 (6x12)
Dimensions	1500x806x35mm (62.2x31.8x1.4inch)
Weight	15.5kg (34.1 lbs.)
Front Glass	3.2mm (0.13inch) tempered glass
Frame	Anodized aluminium alloy
Junction Box	IP65 rated
Output Cables	AWG (12AWG), asymmetrical lengths (-) 1200mm (47.2inch) and (+) 800mm (31.5inch), MC Plug Type N connectors

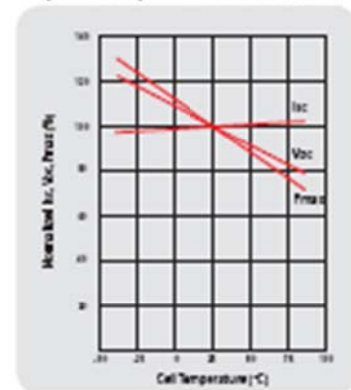
### Temperature Coefficients

Nominal Operating Cell Temperature (NOCT)	45°C±2°C
Temperature Coefficient of Pmax	-0.48 %/°C
Temperature Coefficient of Voc	-0.34 %/°C
Temperature Coefficient of Isc	0.017 %/°C

Current-Voltage & Power-Voltage Curve (170W)



Temperature Dependence of Isc, Voc, Pmax



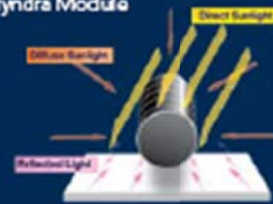



**SOLYNDRA™**  
The new shape of solar™

Solar photovoltaic systems comprised of panels and mounting hardware for low slope, commercial rooftops.

Proprietary cylindrical modules optimize the collection of sunlight and enable Solyndra panels to achieve the highest rooftop coverage without the need for costly mounting hardware or rooftop penetrations. By significantly reducing installation costs and increasing the electricity generated per rooftop, Solyndra delivers electricity at the lowest cost per kilowatt hour.

Solyndra Module

**Significantly more solar electricity per rooftop per year**  
Approximately 2x the roof coverage with no need for tilting and spacing

**Fast, easy, economical installation**  
Typically, 1/3 the labor, 1/3 the time, at 1/2 the cost

**Lightweight and self-ballasting**  
No penetrations or attachments required

# Product Specifications

## Electrical Data

Measured at Standard Test Conditions (STC) irradiance of 1000 W/m<sup>2</sup>, air mass 1.5, and cell temperature 25° C

Model Number		SL-001-150	SL-001-157	SL-001-165	SL-001-173	SL-001-182	SL-001-191	SL-001-200 <small>Release Date TBC</small>
Power Rating (P <sub>max</sub> )	Wp	150 Wp	157 Wp	165 Wp	173 Wp	182 Wp	191 Wp	200 Wp
Power Tolerance (%)	%/Wp	+4, -5	+/-4	+/-4	+/-4	+/-4	+/-4	+/-4
V <sub>mp</sub> (Voltage at Maximum Power)	Volts	65.7 V	67.5 V	69.6 V	71.7 V	73.9 V	76.1 V	78.3 V
I <sub>mp</sub> (Current at Maximum Power)	Amps	2.28 A	2.33 A	2.37 A	2.41 A	2.46 A	2.51 A	2.55 A
V <sub>oc</sub> (Open Circuit Voltage)	Volts	91.4 V	92.5 V	93.9 V	95.2 V	96.7 V	98.2 V	99.7 V
I <sub>sc</sub> (Short Circuit Current)	Amps	2.72 A	2.73 A	2.74 A	2.75 A	2.76 A	2.77 A	2.78 A
Temp. Coefficient of V <sub>oc</sub>	%/°C							-24
Temp. Coefficient of I <sub>sc</sub>	%/°C							-02
Temp. Coefficient of Power	%/°C							-26

## System Information

Cell type	Cylindrical CIGS
Maximum System Voltage	Universal design: 1000V (IEC) & 600V (UL) systems
Dimensions	Panel: 1.82 m x 1.08 m x 0.05 m Height: 0.3 m to top of panel on mounts
Mounts	Non-penetrating, powder-coated Aluminum Up to 2.17 mounts per panel
Connectors	4 Tyco Solarlok; 0.20 m cable
Series Fuse Rating	23 Amps
Roof Load	16 kg/m <sup>2</sup> (3.3 lb/ft <sup>2</sup> ) panel and mounts
Panel Weight	31 kg (68 lb) without mounts
Snow Load Maximum	2800 Pa (58.5 lb/ft <sup>2</sup> )
Wind Performance	208 km/h (130 mph) maximum Self-ballasting with no attachments
Operating and Storage Temp	-40°C to +85°C
Normal Operating Cell Temperature (NOCT)	41.7°C at 800 W/m <sup>2</sup> , Temp = 20°C, Wind = 1m/s
Certifications/Listings	UL1703, IEC 61646, CEC listing IEC 61730, IEC 61646, CE Mark Application Class A per IEC 61730-2 Fire Class C
Warranty	25 year limited power warranty 5 year limited product warranty

Specifications subject to change without notice.

Solyndra, Inc. • 47700 Kato Road • Fremont, CA • [www.solyndra.com](http://www.solyndra.com)

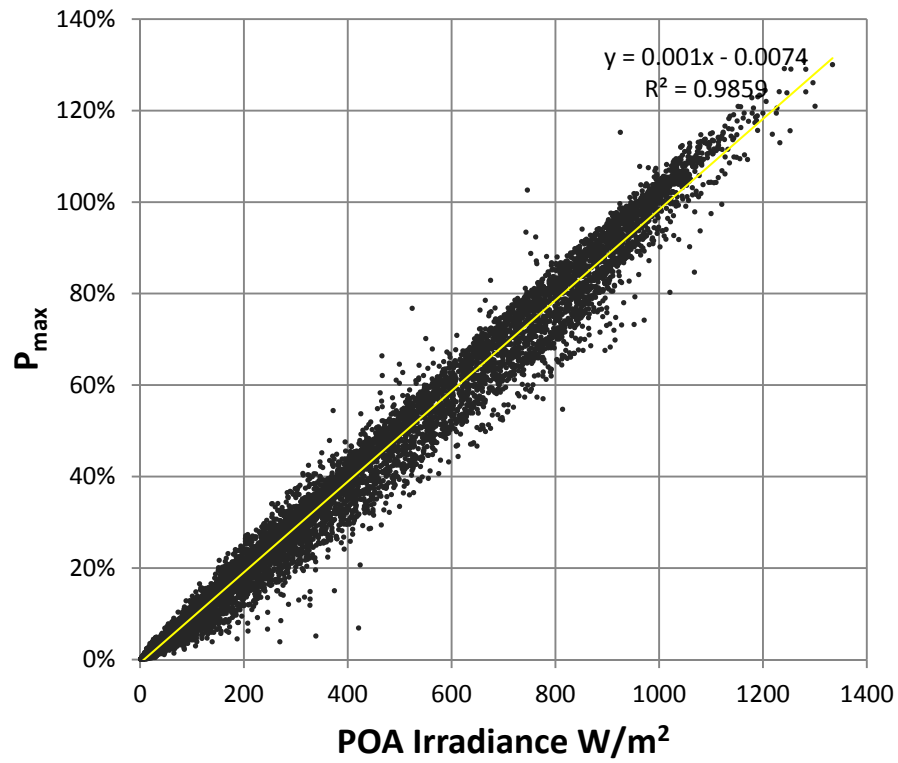


Solyndra's panels come with all of the mounts, grounding connectors, lateral clips, and fasteners required to build a standard array.

**SOLYNDRA**<sup>™</sup>  
The new shape of solar<sup>™</sup>

## Appendix 5: a-Si module Results

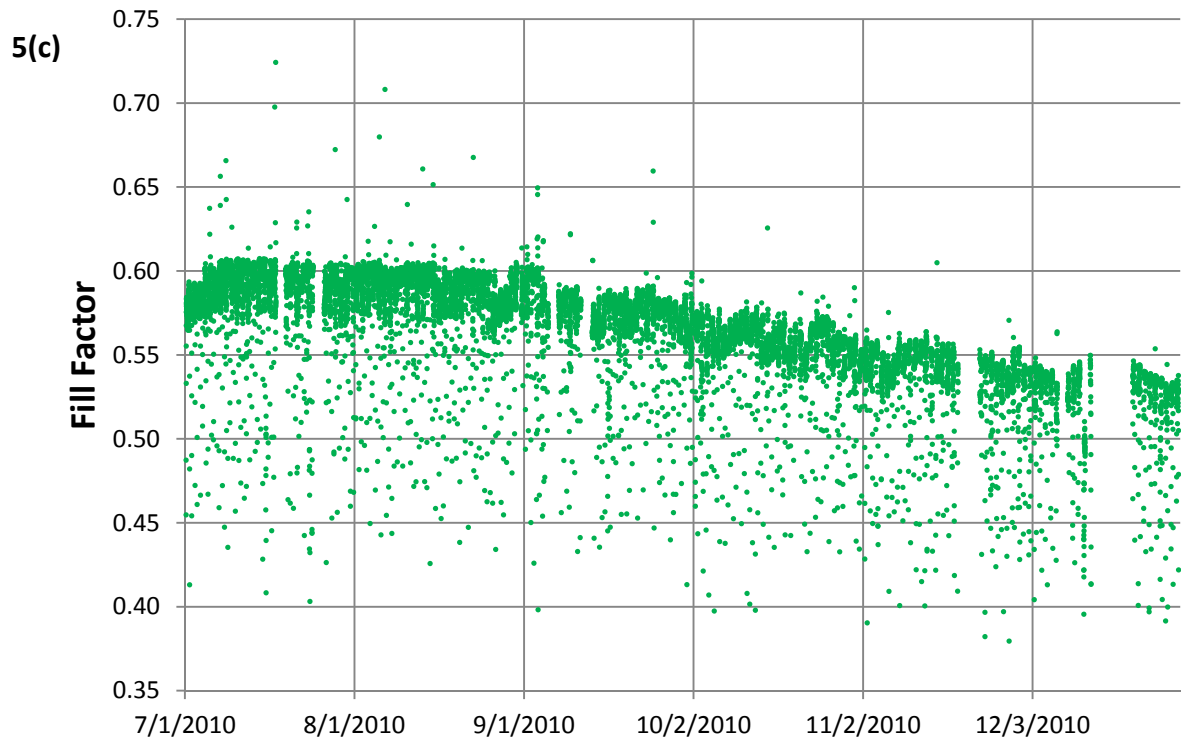
5(a)



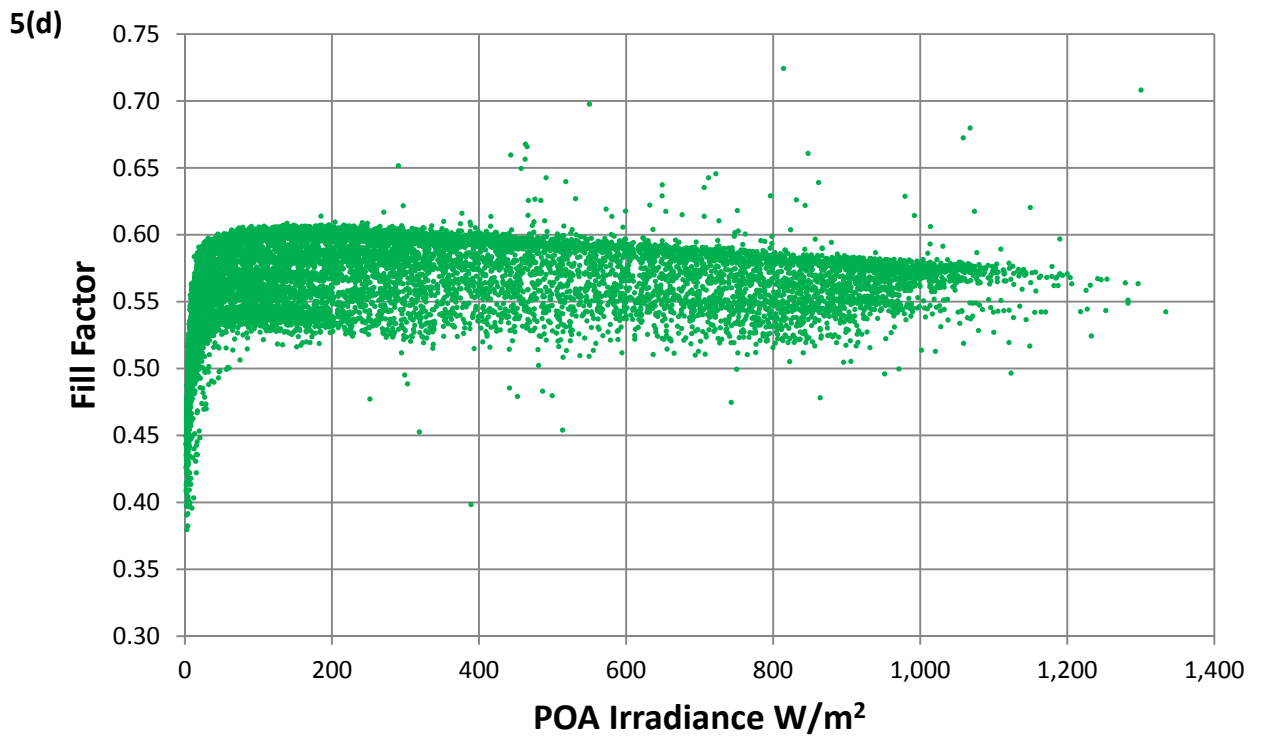
5(b)



a-Si module fill factor over time and POA Irradiance

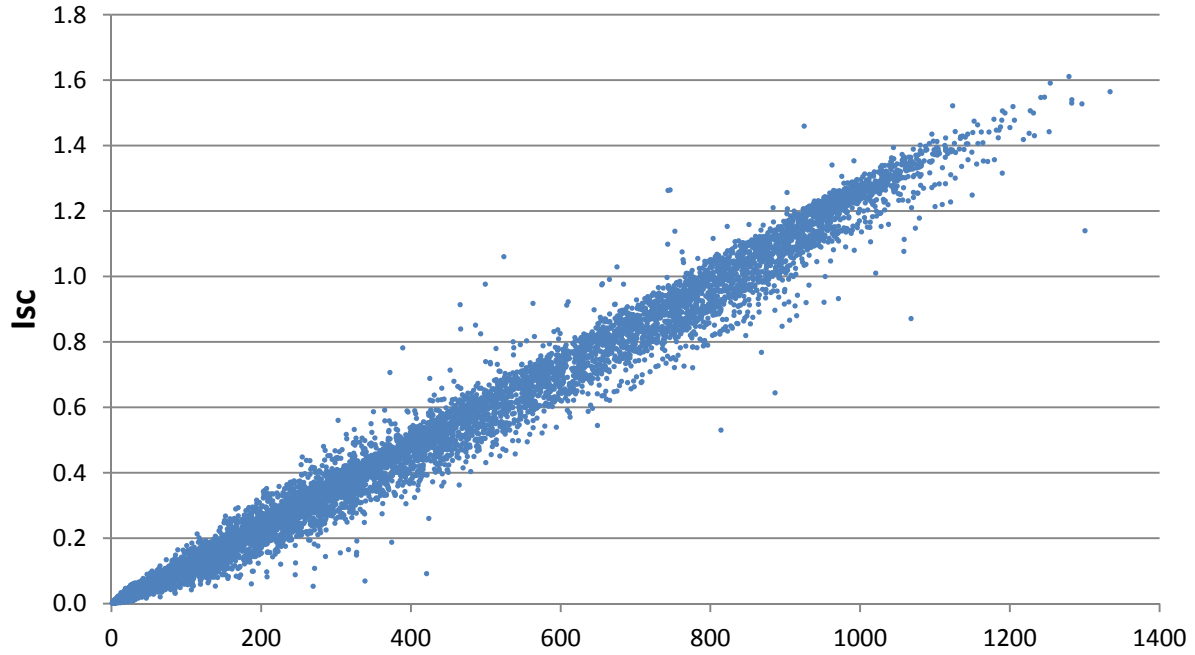


Note the drop in efficiency (fill factor) during colder months (above).

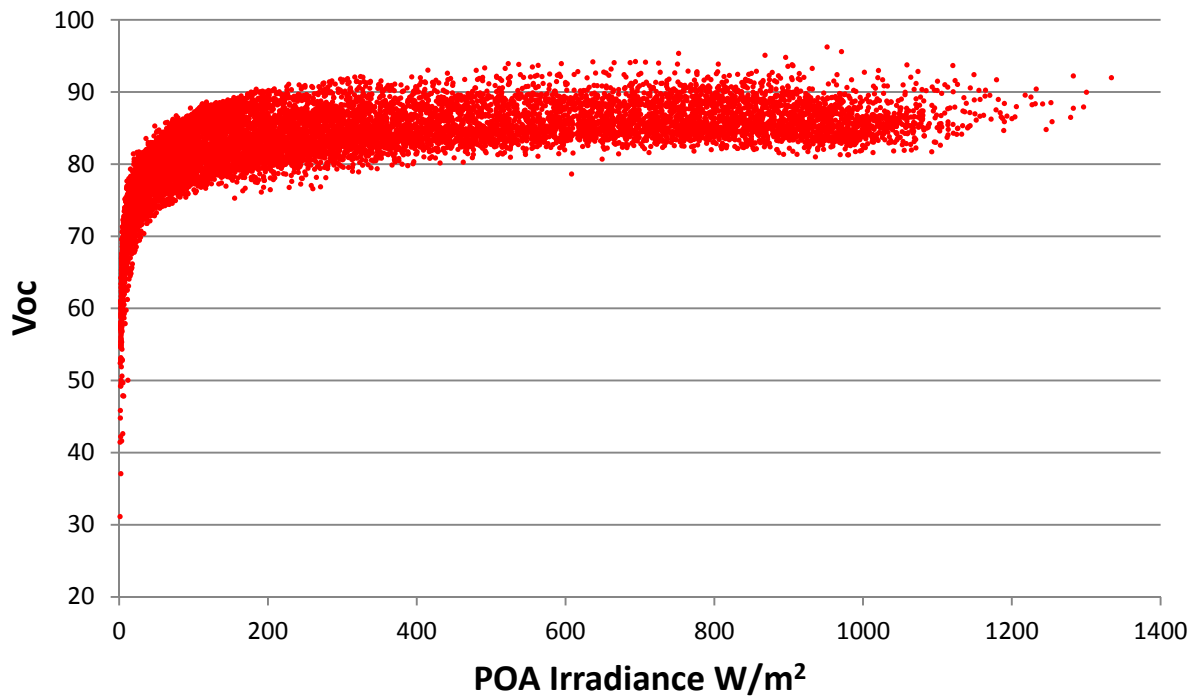


a-Si module electrical characteristics – current (I) and voltage (V) versus POA Irradiance

5(e)



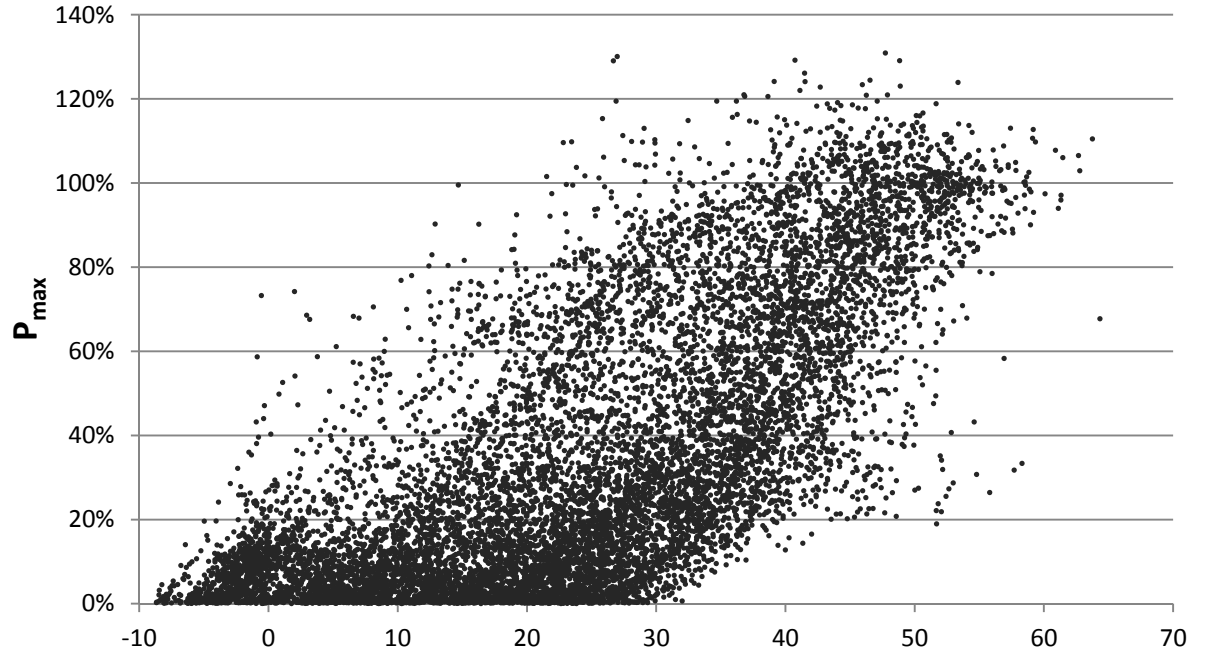
5(f)



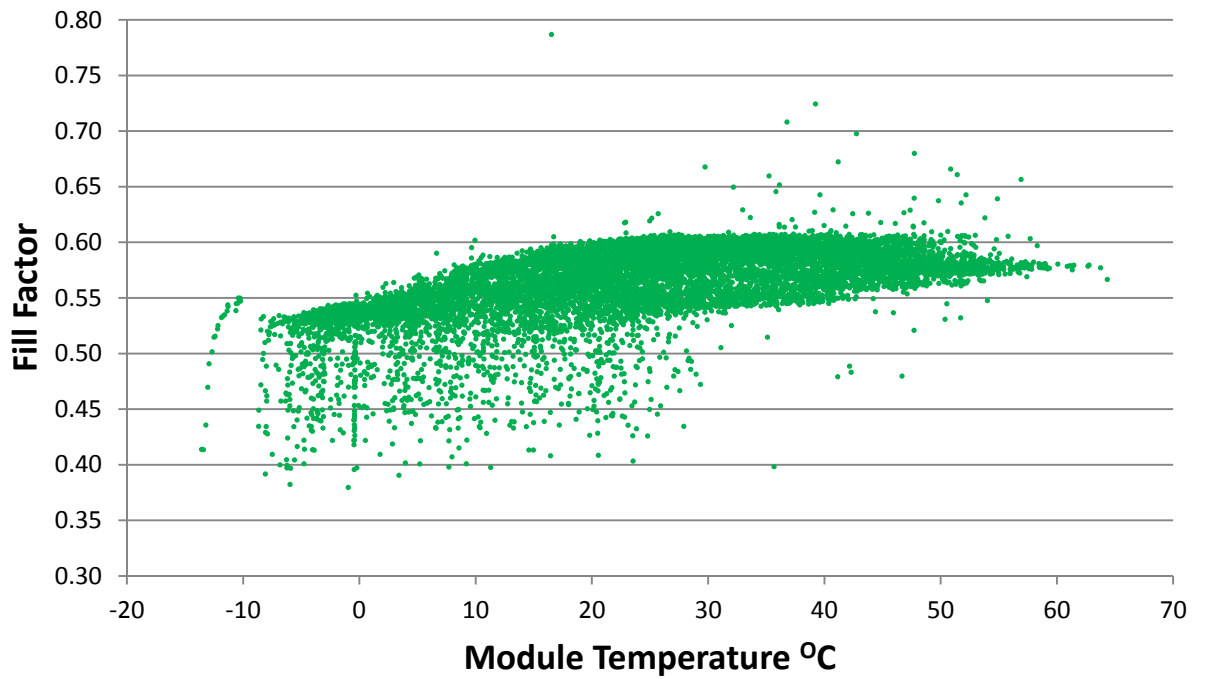


## a-Si module Power and Efficiency versus Module Temperature

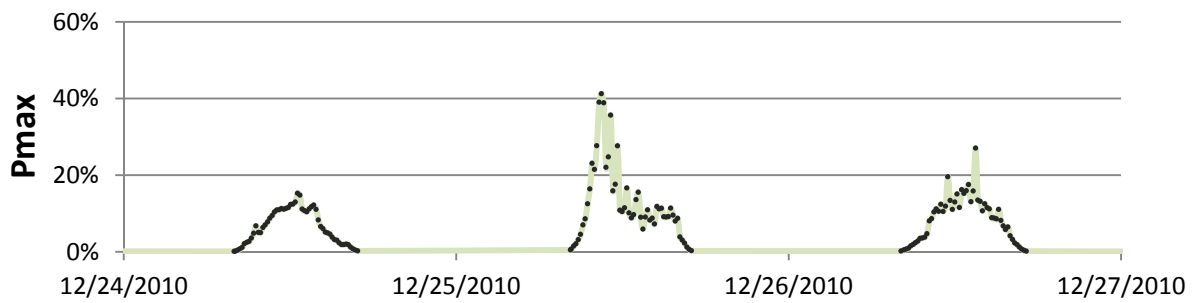
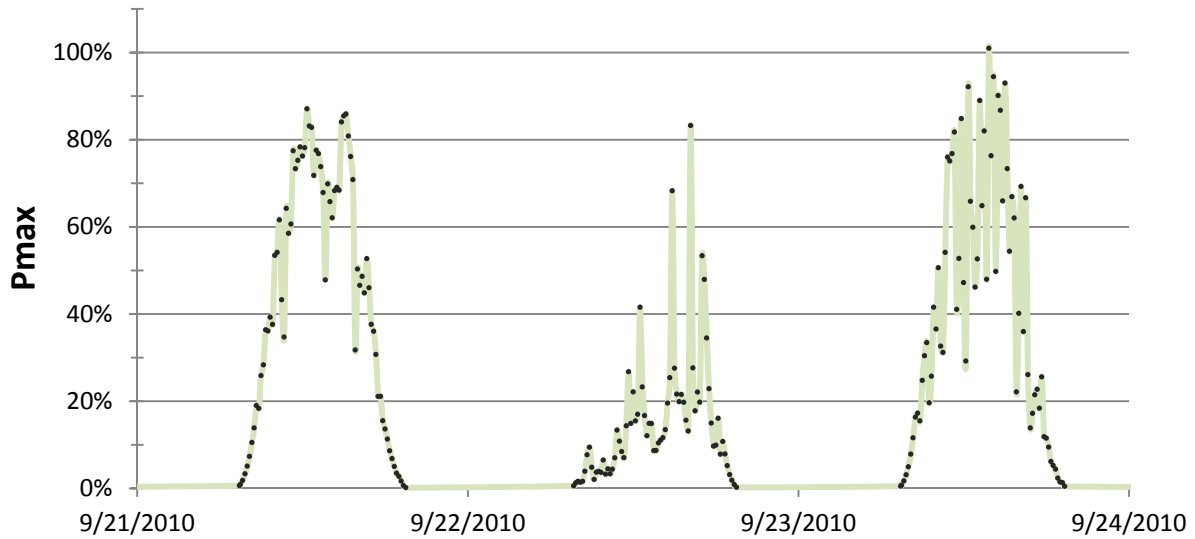
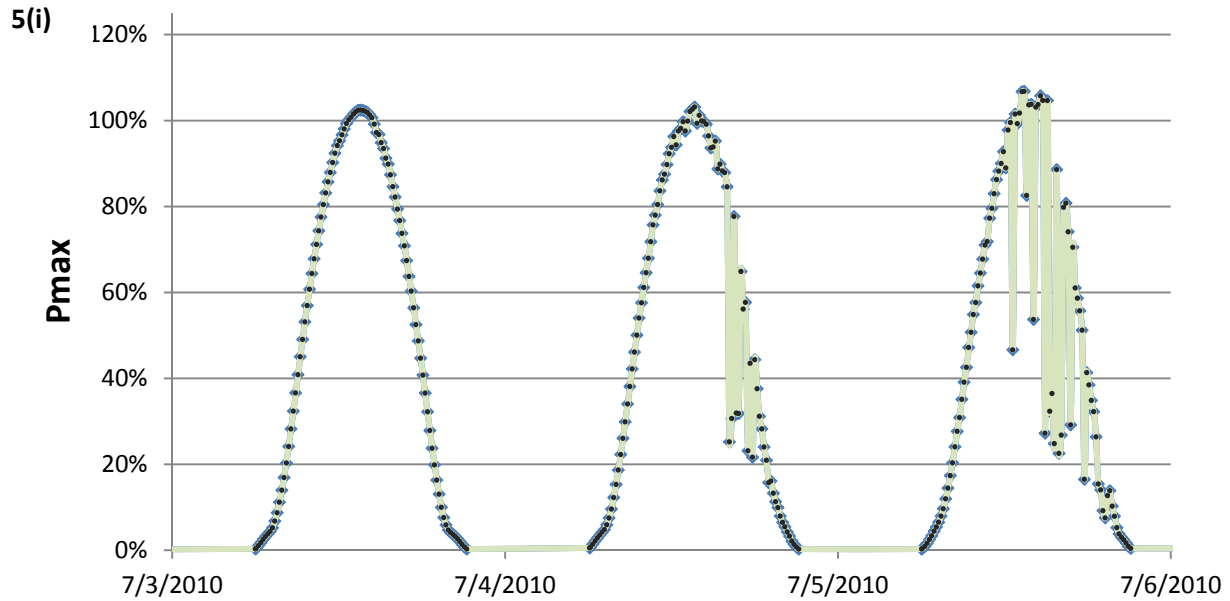
5(g)



5(h)

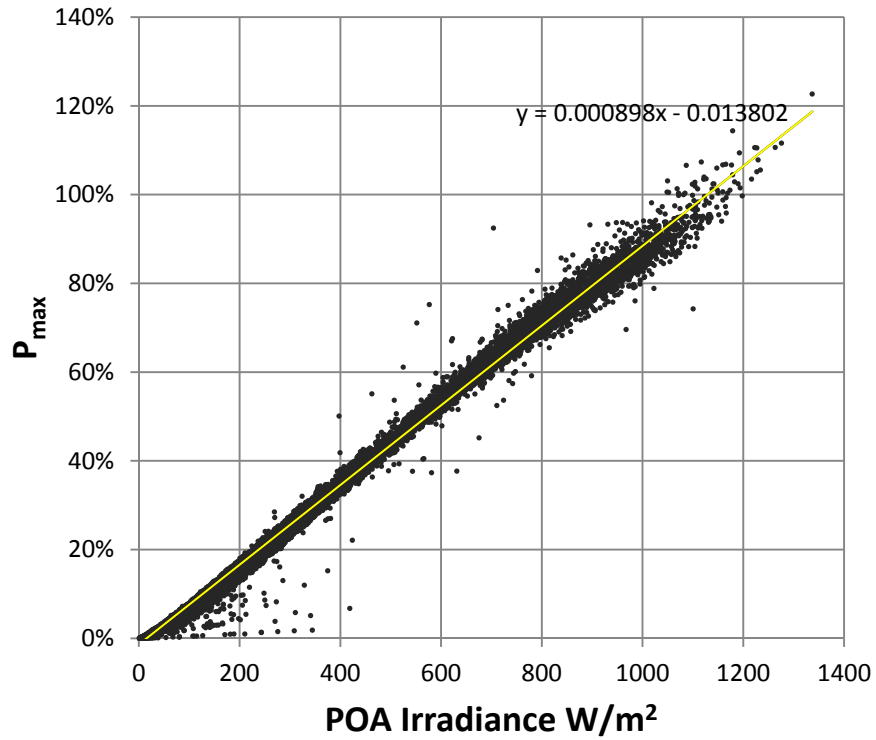


a-Si module Energy yields for three concurrent days in July, Sept and Dec 2010



## Appendix 6: c-Si module Results

6(a)

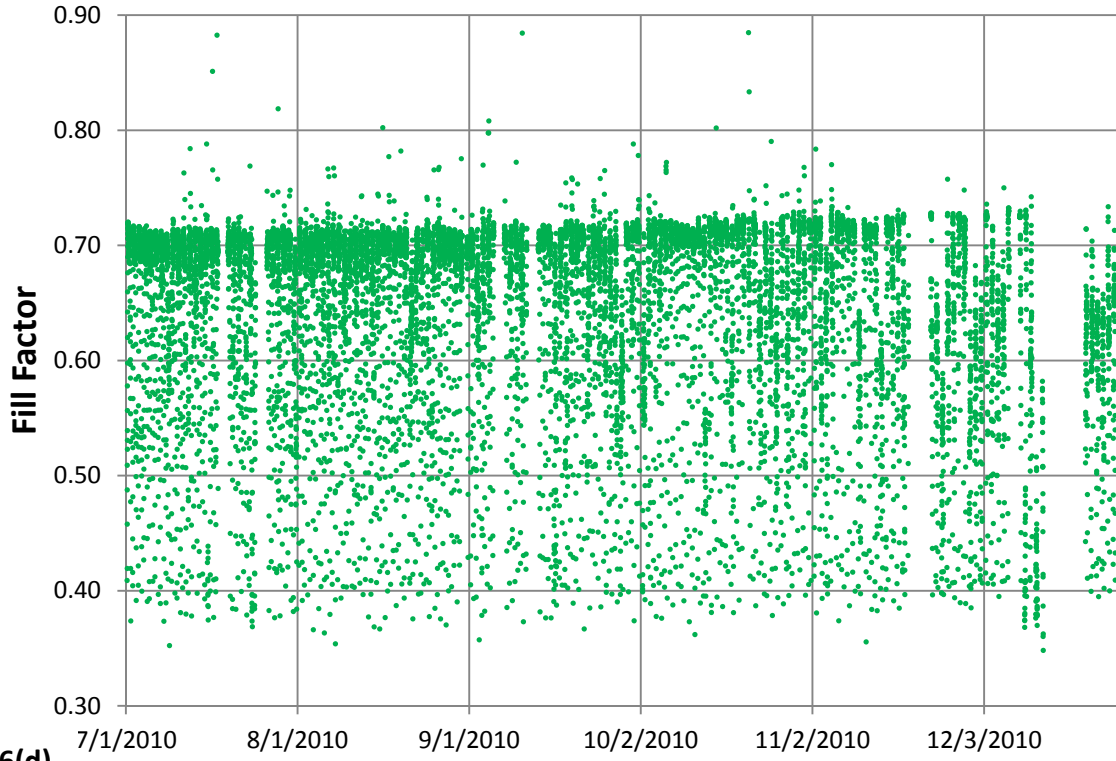


6(b)

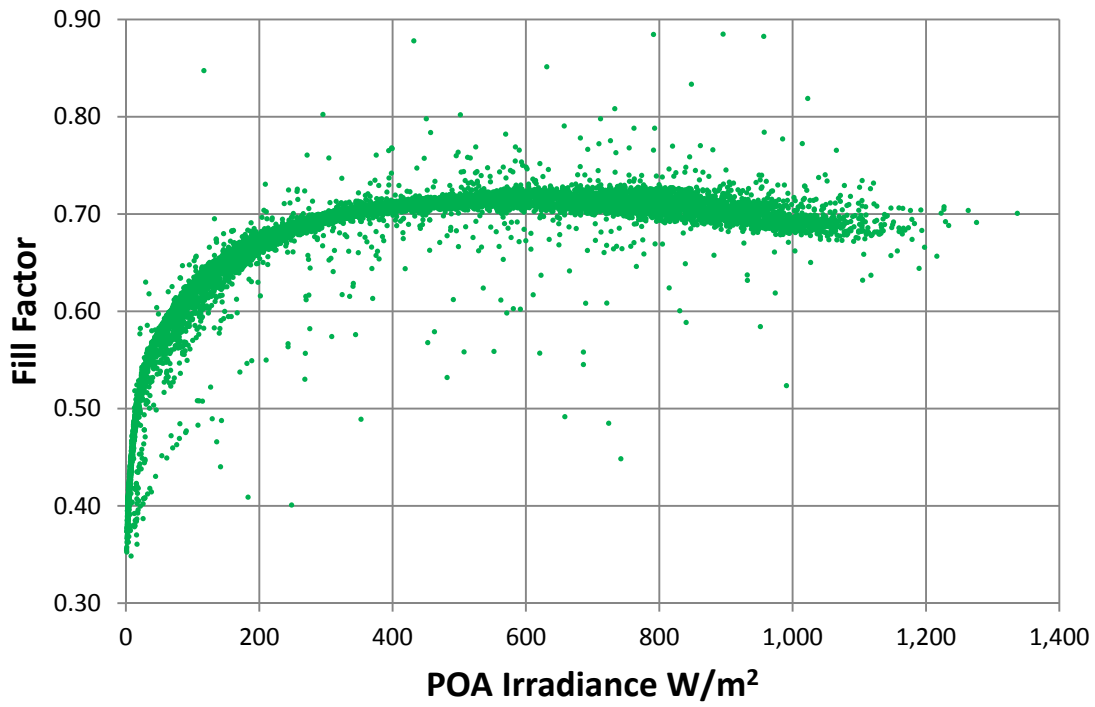


c-Si module fill factor

6(c)

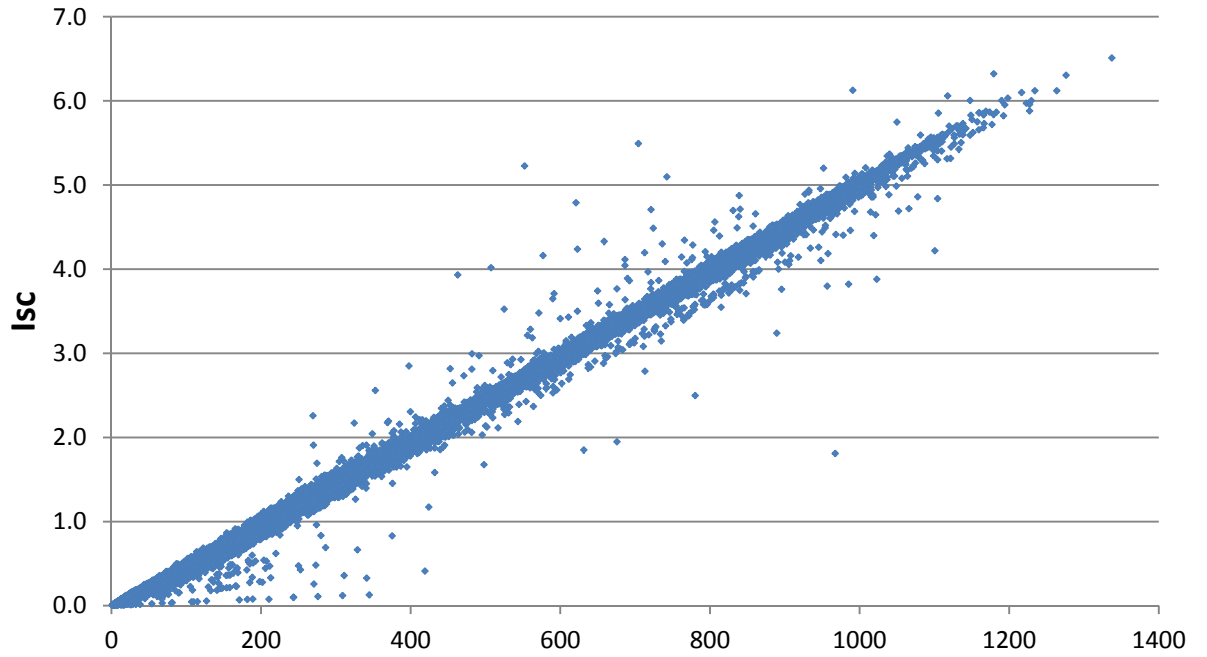


6(d)

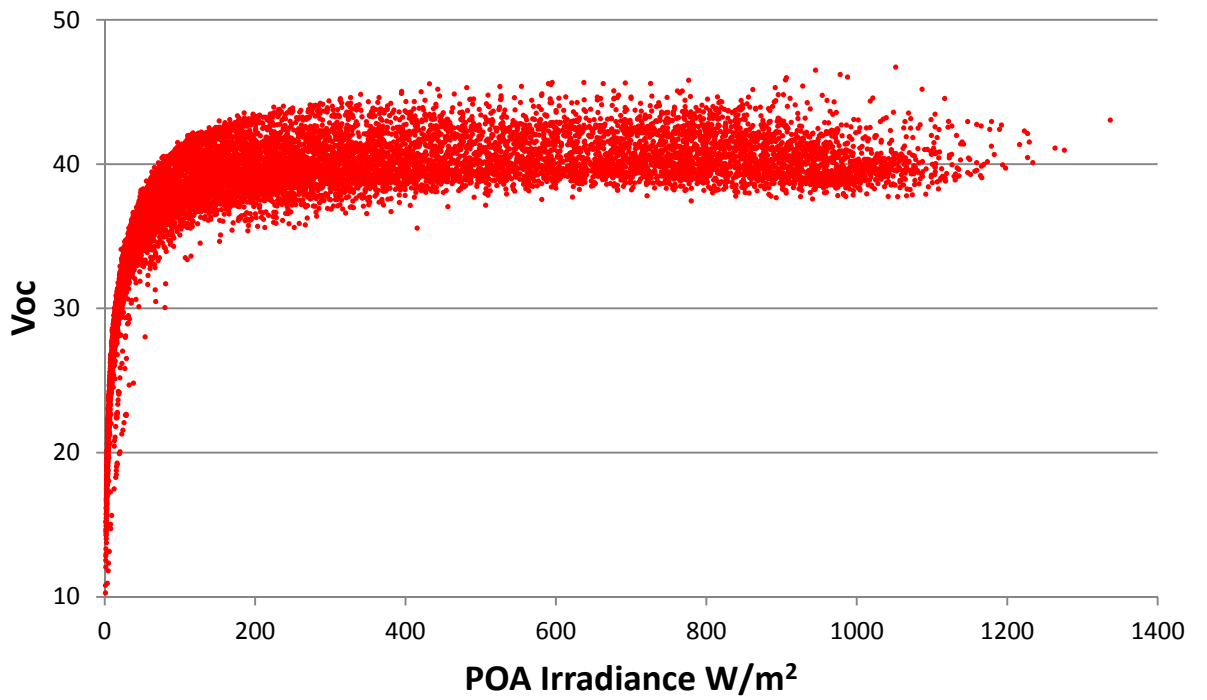


c-Si module electrical characteristics - current (I) and voltage (V) versus POA Irradiance

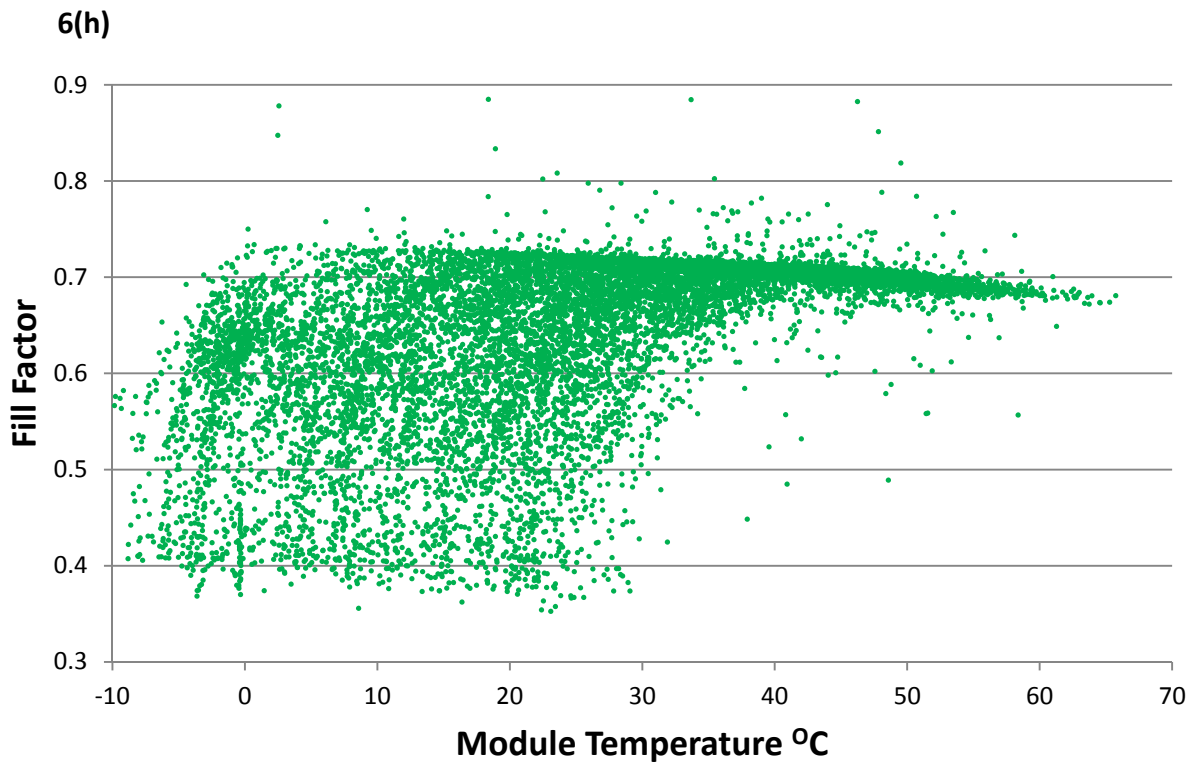
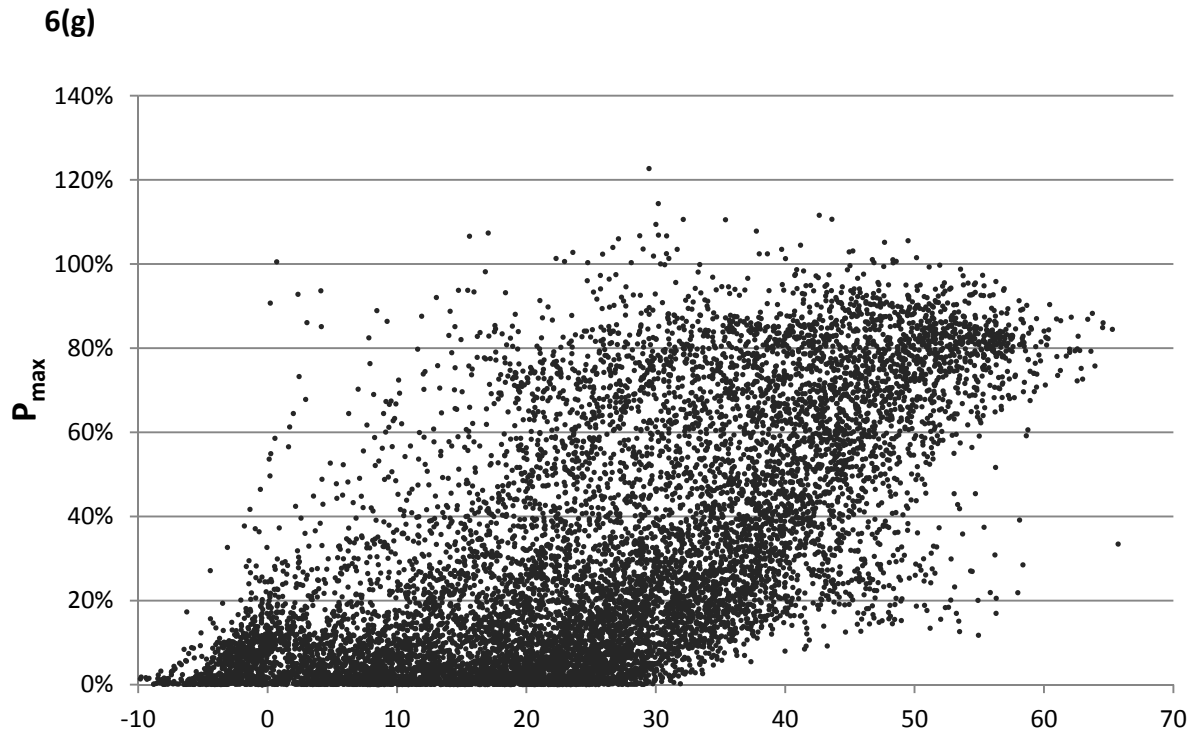
6(e)



6(f)

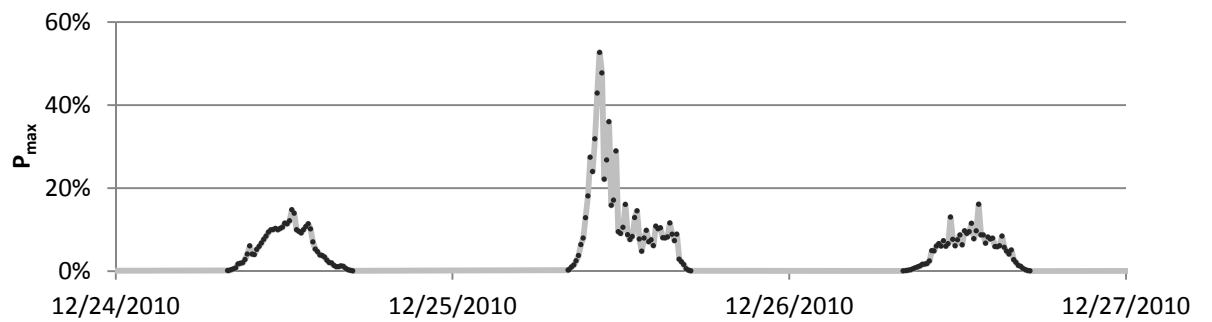
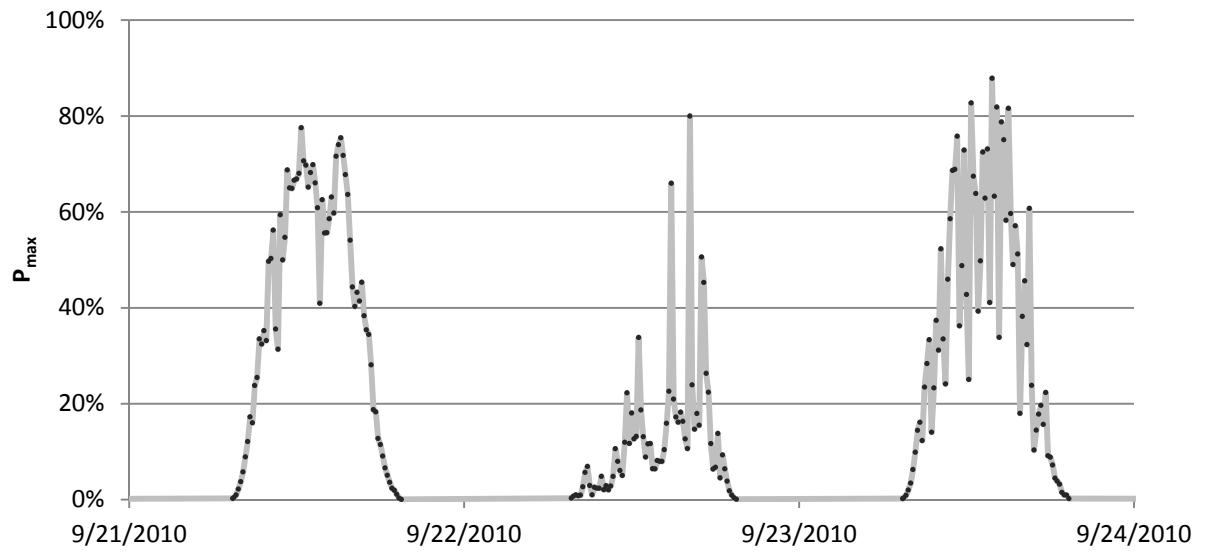
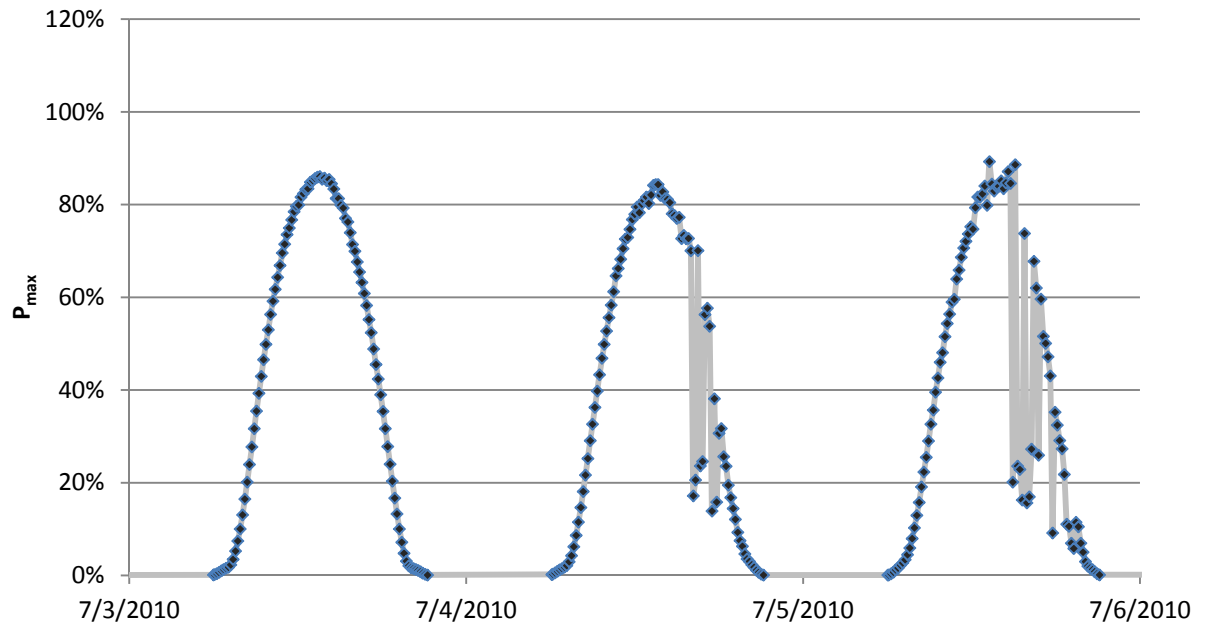


## c-Si module Power and Efficiency versus Module Temperature



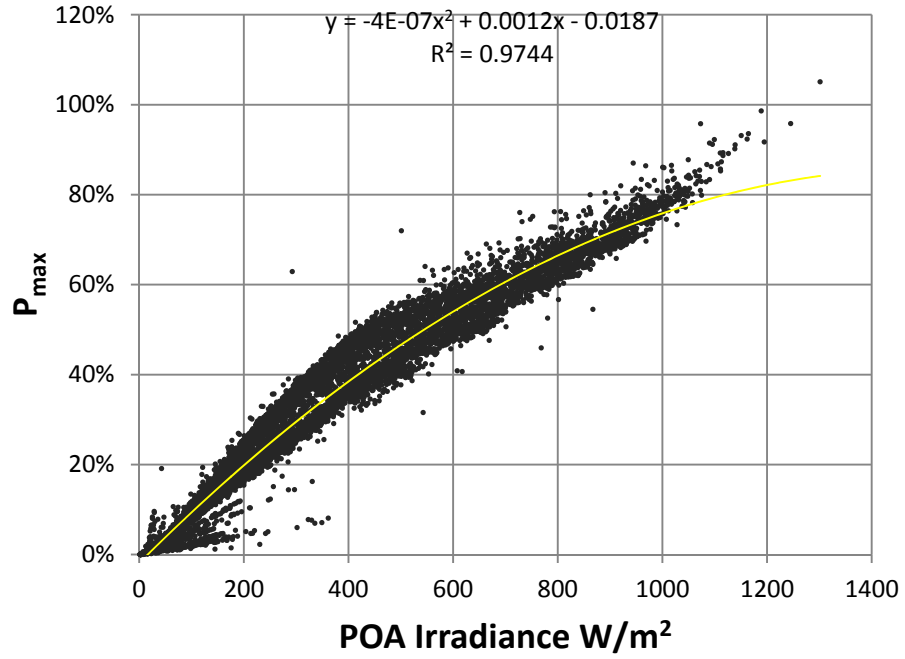
c-Si module Energy yields from three concurrent days in July, Sept and Dec 2010

6(i)



## Appendix 7: CIGS module Results

7(a)

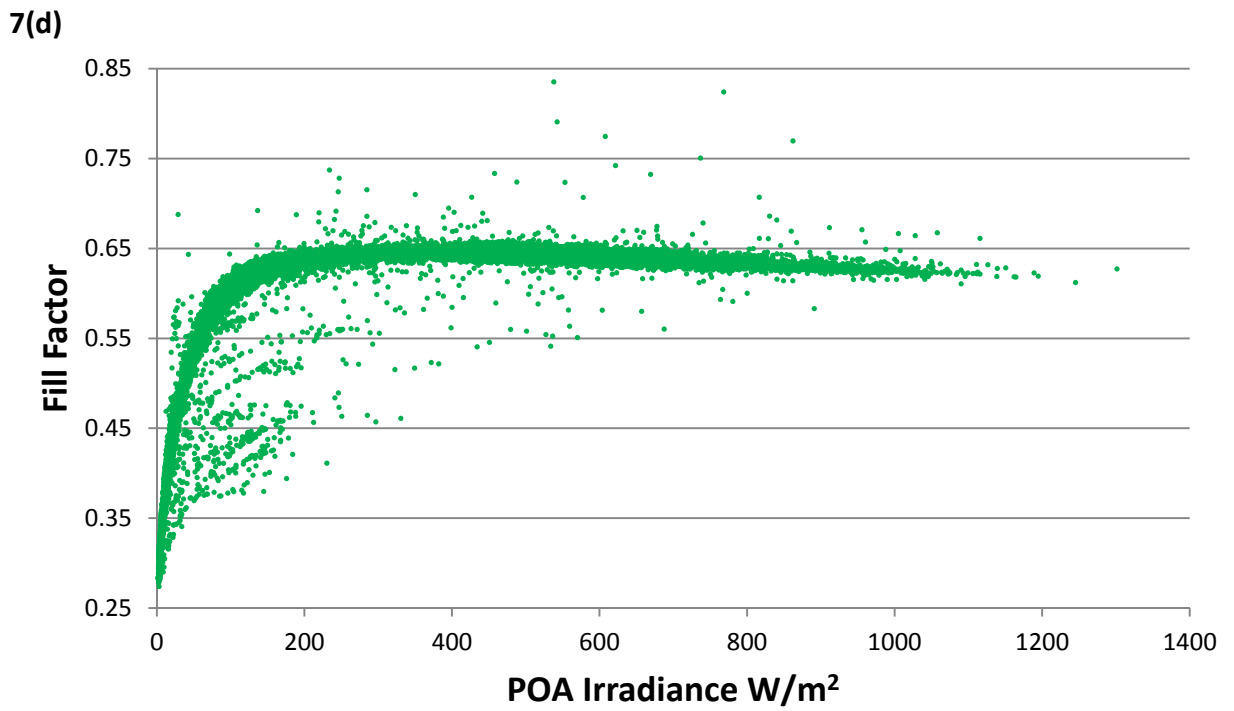
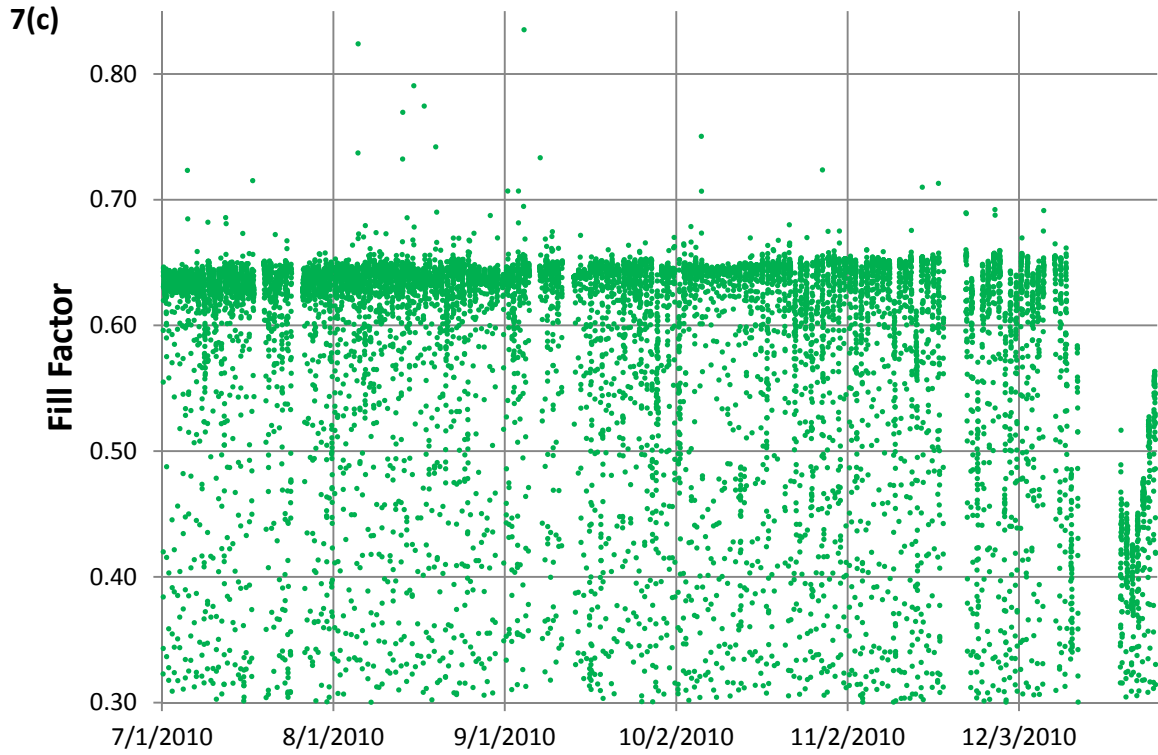


7(b)



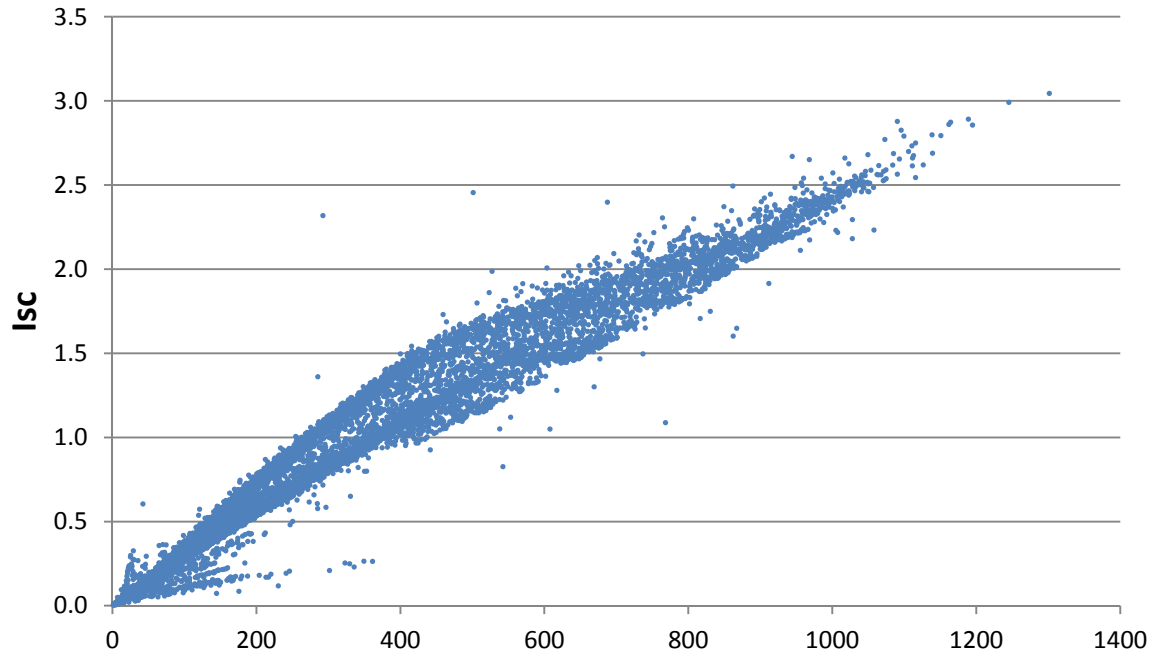


CIGS module fill factor over time and intensity of light (POA Irr)

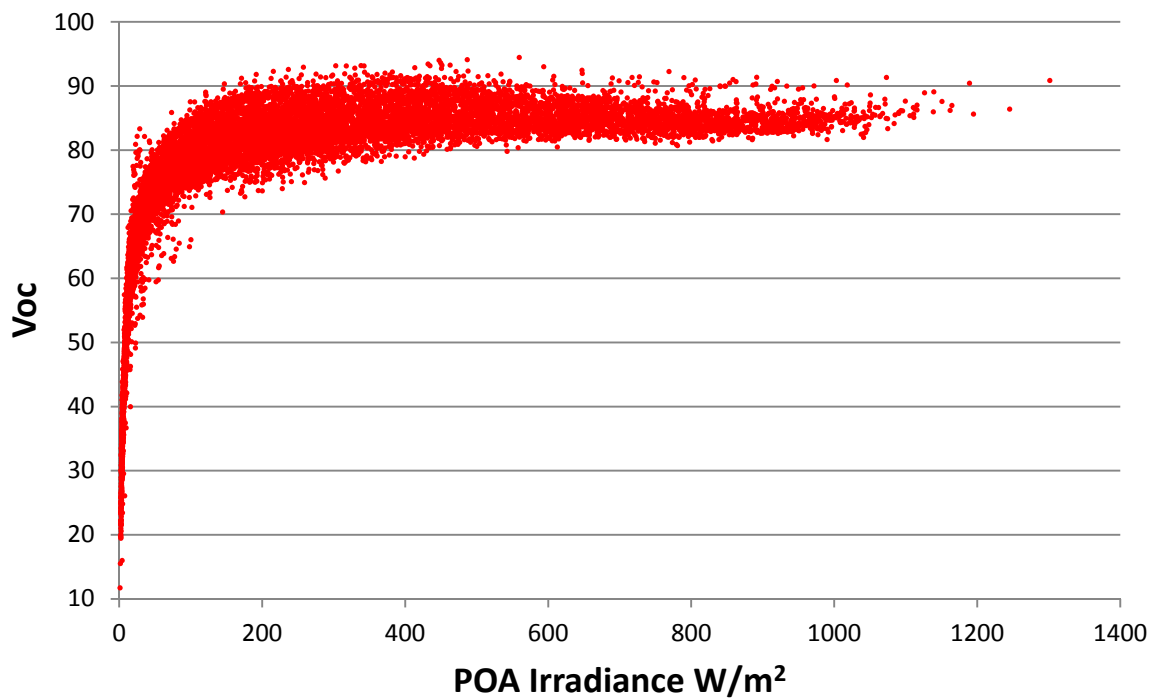


## CIGS module electrical characteristics - current (I) and voltage (V) versus POA Irradiance

7(e)

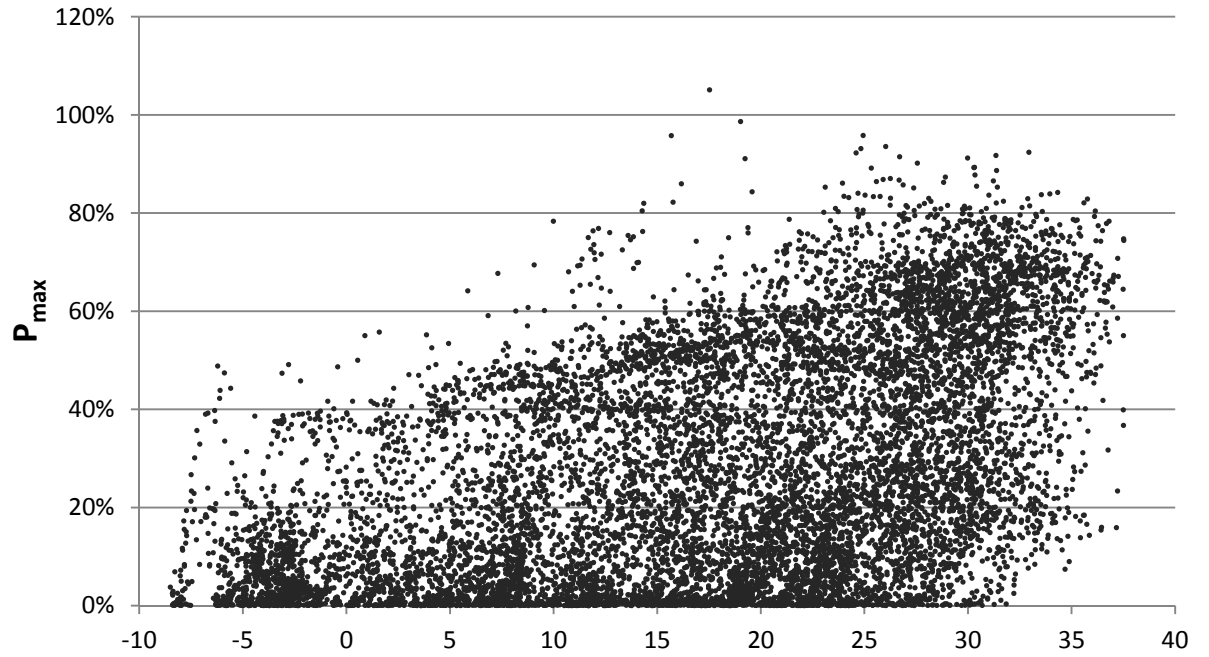


7(f)

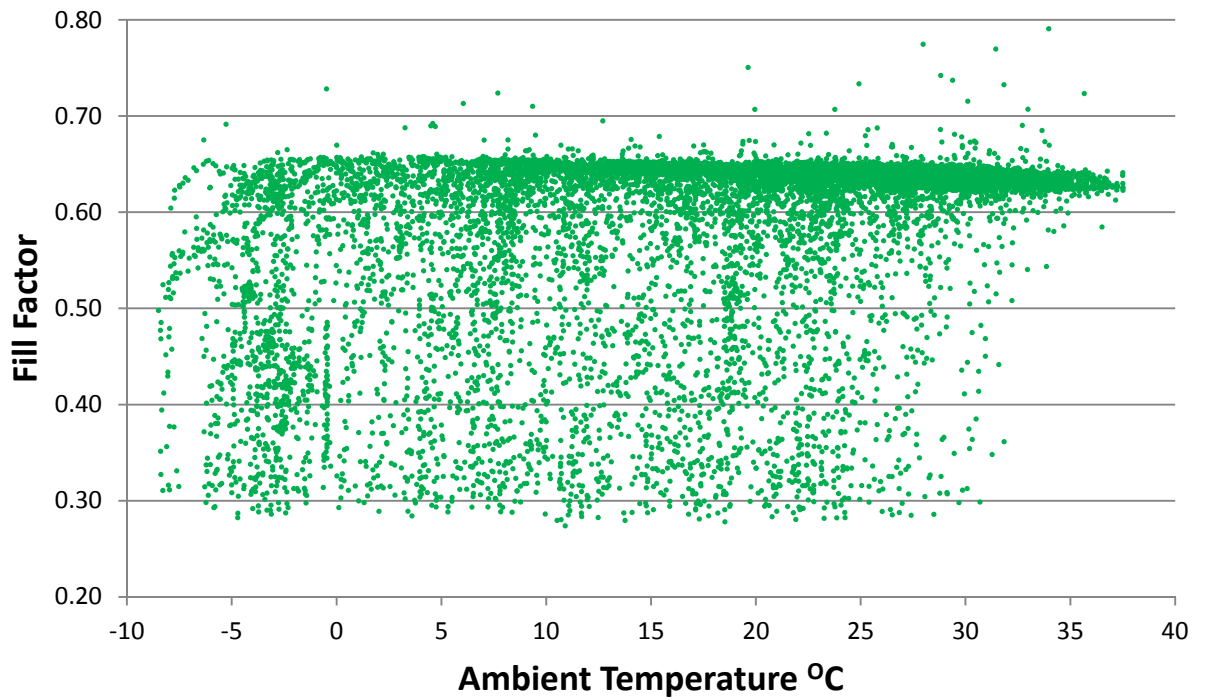


## CIGS module Power and Efficiency versus Ambient Temperature

7(g)

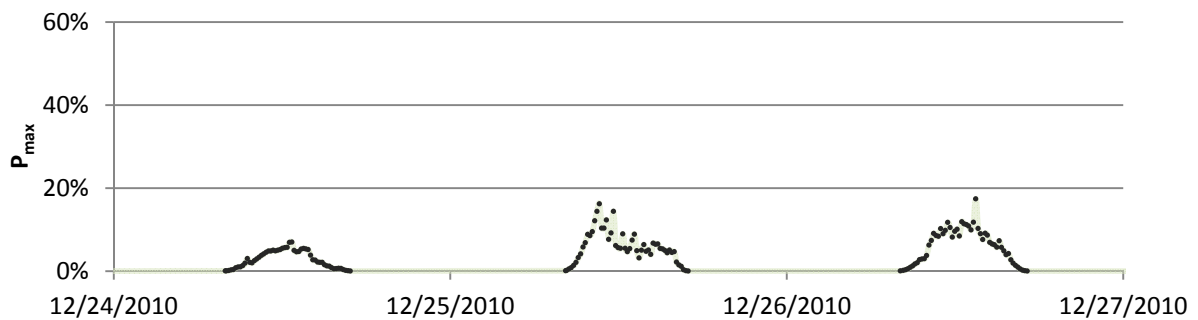
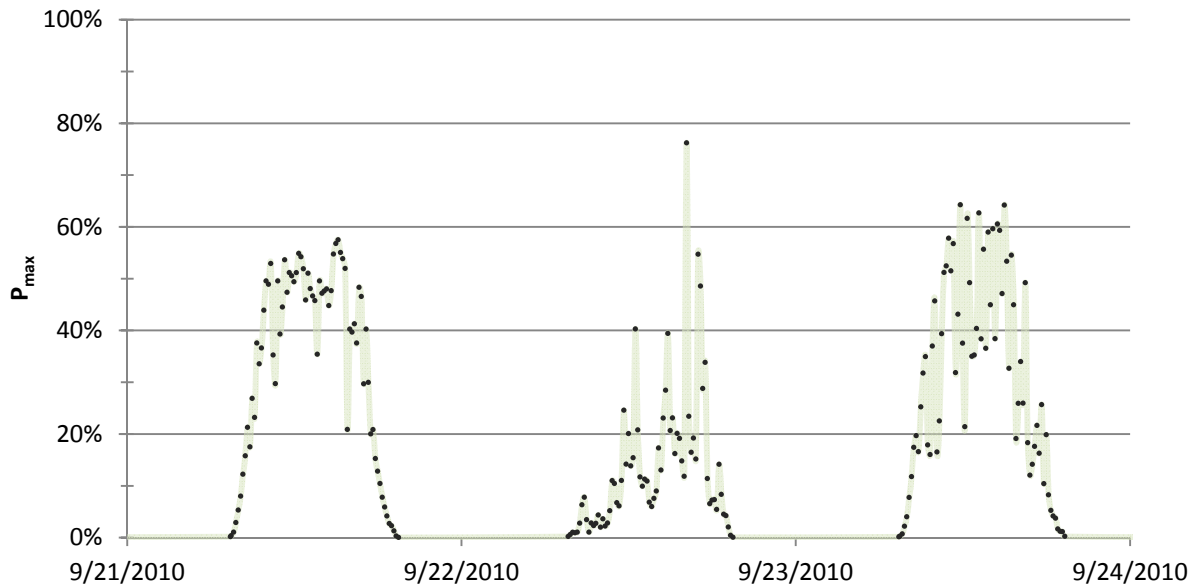
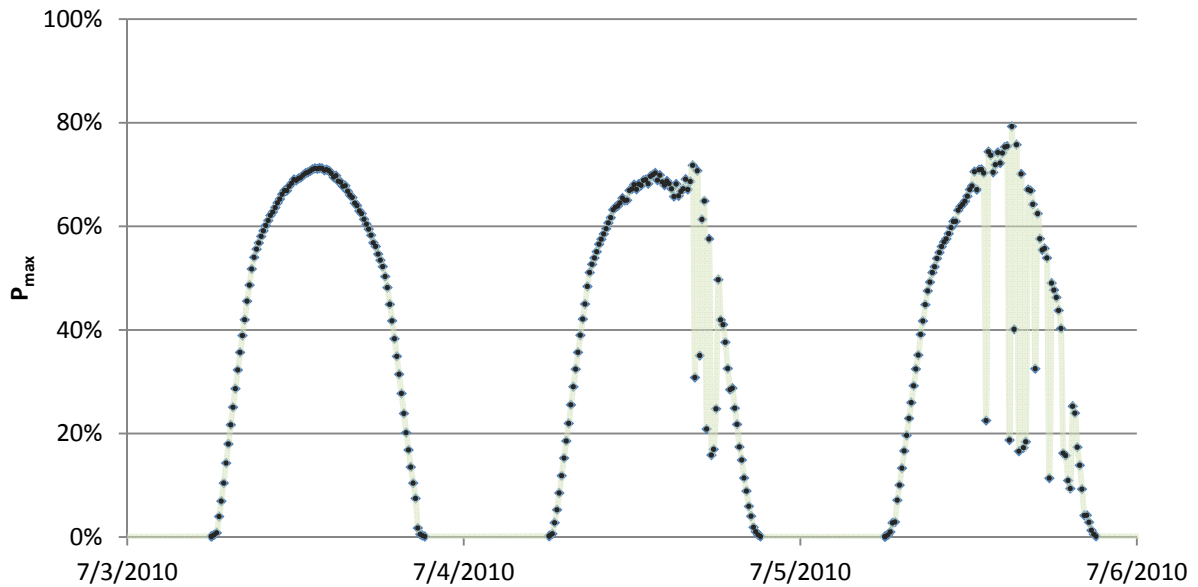


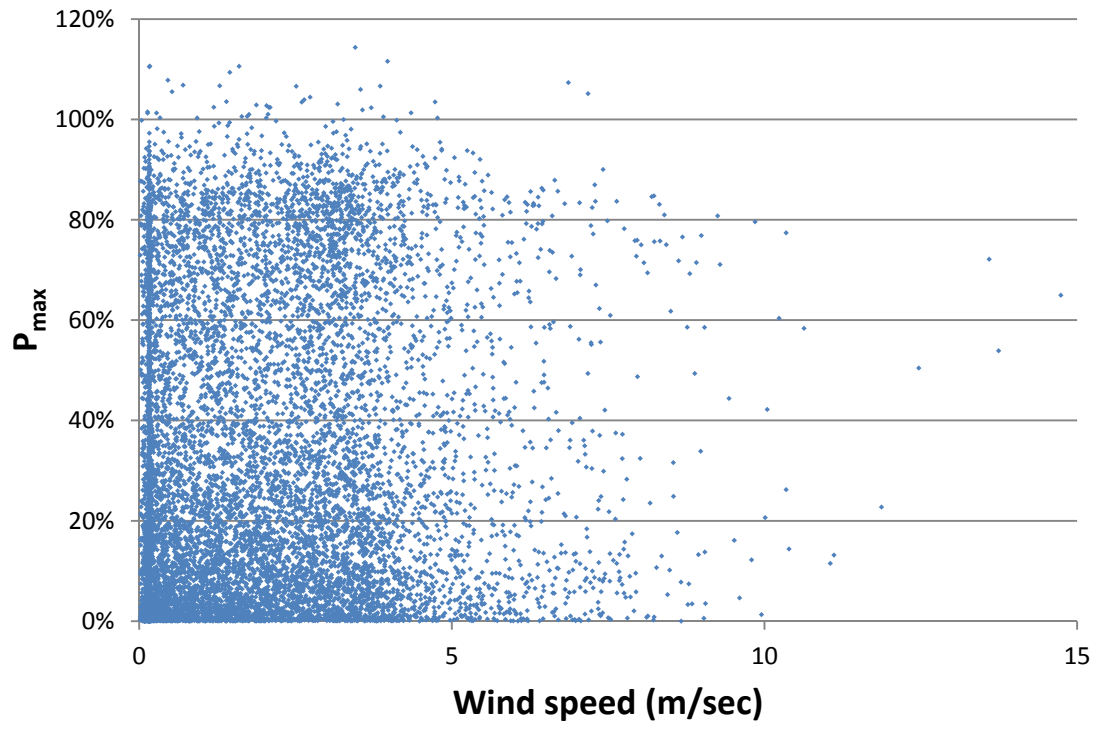
7(h)



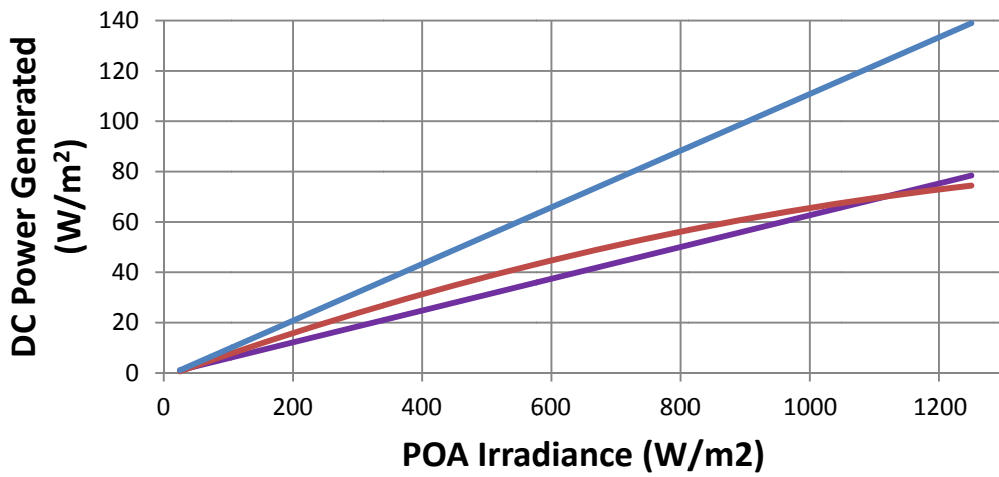
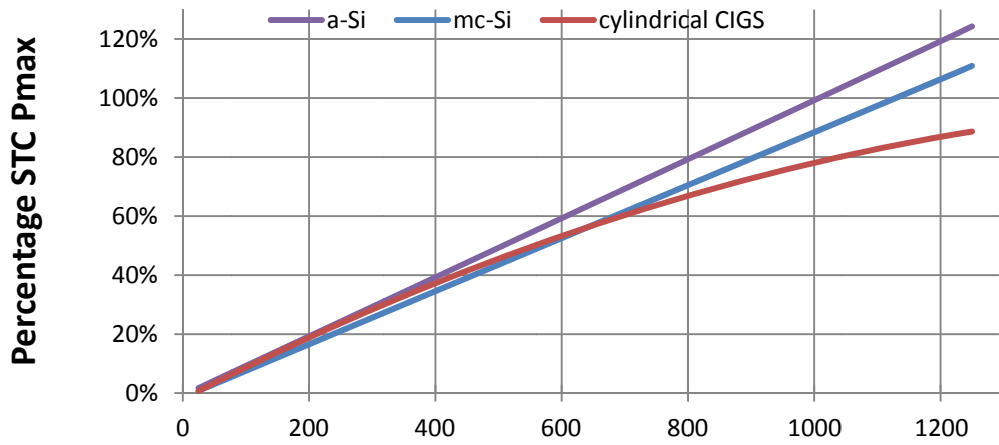
CIGS module Energy yields from three concurrent days in July, Sept and Dec 2010

7(i)

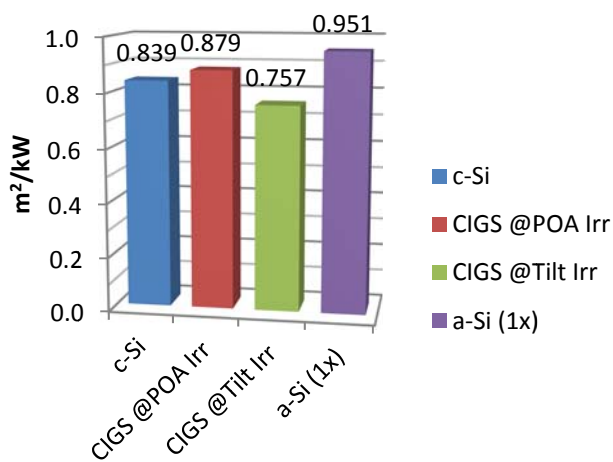


**Appendix 8: Power versus wind speed c-Si module**

Appendix 9: Conclusions



Whr/(Irr kWhr/m²)/STC P<sub>max</sub>



Whr/(Irr kWhr/m²)

